

128

FINITE ELEMENT ANALYSIS OF TRIMMING PROCESS

**A THESIS SUBMITTED TO
THE GRADUATE SCHOOL OF NATURAL AND APPLIED SCIENCES
OF
THE MIDDLE EAST TECHNICAL UNIVERSITY**

BY

SERDAR Ş. İSBİR

118990


**T.C. YÜKSEKÖĞRETİM KURULU
DOKÜMANTASYON MERKEZİ**

118990

**IN PARTIAL FULFILLMENT OF THE REQUIREMENTS FOR THE
DEGREE OF
MASTER OF SCIENCE
IN
THE DEPARTMENT OF MECHANICAL ENGINEERING**


OCTOBER 2002

Approval of the Graduate School of Natural and Applied Sciences.



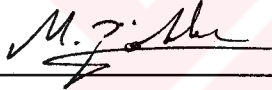
Prof. Dr. Tayfur ÖZTÜRK
Director

I certify that this thesis satisfies all the requirements as a thesis for the degree of Master of Science.



Prof. Dr. Erez SÖYLEMEZ
Head of the Department

This is to certify that we have read this thesis and that in our opinion it is fully adequate, in scope and quality, as a thesis for the degree of Master of Science.



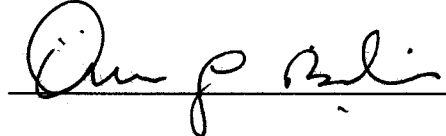
Prof. Dr. Mustafa İlhan GÖKLER
Co-supervisor



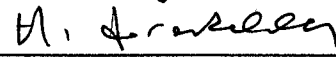
Prof. Dr. Haluk DARENDELİLER
Supervisor

Examining Committee Members:

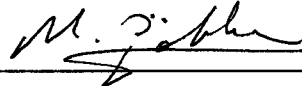
Prof. Dr. Ömer G. BİLİR



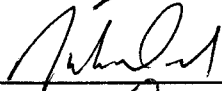
Prof. Dr. Haluk DARENDELİLER



Prof. Dr. Mustafa İlhan GÖKLER



Prof. Dr. Suha ORAL



Prof. Dr. Can ÇOĞUN



ABSTRACT

FINITE ELEMENT ANALYSIS OF TRIMMING PROCESS

İSBİR, Serdar Ş.

M.S., Department of Mechanical Engineering

Supervisor: Prof. Dr. Haluk DARENDELİLER

Co-supervisor: Prof. Dr. Mustafa İlhan GÖKLER

October 2002, 116 pages

Trimming is a commonly used operation in metal cutting, sheet metal forming, blanking, and flash removal in cast and forged parts. It is basically a shearing operation in which adjacent parts of a material is separated through controlled fracture. Finite element simulation of trimming is a highly non-linear and complex process involving crack initiation and propagation and material separation analysis.

This study focuses on the finite element simulation of shearing using the element elimination method. Two failure criteria; shear strain energy density and effective plastic strain were used together with the developed element elimination algorithm to predict failure. Simulation results were verified with tension tests at room temperature.

A forged part was chosen from industry to analyze the trimming operation. Stress distribution and concentration were determined to modify the die set used in the production. A modification for the dies was proposed. High quality parts

were successfully produced with the modified die and lifetime of trimming dies were increased.

Keywords: Trimming, Forging, Shearing, Finite Element Method



ÖZ

ÇAPAK KESME İŞLEMİNİN SONLU ELEMAN METODU İLE ANALİZİ

İSBİR, Serdar

Yüksek Lisans, Makine Mühendisliği Bölümü

Tez Yöneticisi: Prof. Dr. Haluk DARENDELİLER

Ortak Tez Yöneticisi: Prof. Dr. Mustafa İlhan GÖKLER

Ekim 2002, 116 sayfa

Çapak kesme işlemi, metal kesme, saç metal şekillendirme, delme, dövme ve döküm parçalarında sıklıkla kullanılır. Çapak kesme işleminde malzeme kontrollü bir koparma işlemiyle ikiye ayrılır. Kesme işleminin sonlu eleman metodu ile analizi, çatlak oluşumu, ilerlemesi ve malzeme kırılmasını kapsayan, doğrusal olmayan ve karmaşık bir konudur.

Bu çalışma kesme işleminin eleman yoketme metodu ile analizi üzerine yoğunlaşmaktadır. Kopma kriteri olarak gerilme enerjisi yoğunluğu ve plastik deformasyon, geliştirilen eleman yoketme algoritması ile birlikte kullanılmıştır. Sonuçlar oda sıcaklığında çekme deneyleri ile doğrulanmıştır.

Kesme işleminin analizi için sanayiden bir parça seçilmiştir. Üretimde kullanılan kalıplardaki gerilim dağılımı belirlenmiştir ve iyileştirme için yeni bir değişiklikler önerilmiştir. Değişiklik yapılan kalıplarda yüksek kalitede parçalar üretilmiş ve kesme kalıplarının kullanım ömrü uzatılmıştır.

Anahtar Kelimeler: Çapak Kesme, Dövme, Sonlu Eleman Metodu



To My Family . . .

ACKNOWLEDGEMENTS

First of all I would like to thank to my supervisors Prof. Dr. Haluk DARENDELİLER and Prof. Dr. Mustafa İlhan GÖKLER for giving me the opportunity to prepare this thesis, their relentless efforts, guidance, and patience.

Next, I am grateful to Mr. Kürşat KAYATÜRK for his valuable support and friendship. His help gave me the strength to continue in my desperate moments. This thesis would not be completed without his help.

Thanks go to helpful friends in METU CAD/CAM and Robotics Research Center. Their help in preparing 3D models in Pro/Engineer added valuable to my study.

I would also like to express my thanks to the owners and active members of AKSAN Corp. for their interest to my study, support, and valuable time.

Thanks go to the members of METU Metallurgical and Materials Engineering Department, especially to Prof. Dr. Bilgehan ÖGEL for providing the opportunity to use their department's facilities and resources, and Research Assistant Nevzat AKGÜN for helping in the high temperature tension tests.

Special thanks go to BİAS A.Ş. for their help in solving the problems encountered in the simulation program.

I am grateful to my family for their encouragement and continuous support.

Finally, thanks go to all the people who were not mentioned here but contributed directly or indirectly to the creation of this study.

TABLE OF CONTENTS

ABSTRACT	iii
ÖZ	v
DEDICATION	vi
ACKNOWLEDGEMENTS	vii
TABLE OF CONTENTS	viii
LIST OF FIGURES	xi
CHAPTER	
1. INTRODUCTION	1
1.1 Survey of Previous Literature	3
1.1.1 Applications of Shearing Simulation in Manufacturing Operations	5
1.1.2 Failure Criteria Used in Shearing Analysis	8
1.1.3 Influence of Input Variables on the Trimming Operation	12
1.1.4 Finite Element Simulation	14
1.2 Scope of This Study	16
2. TRIMMING PROCESS	18
2.1 Trimming Operation	18
2.2 Mechanics of Shearing	19
2.3 Factors Affecting Shearing	20
2.3.1 Clearance	20

2.3.2	Force Required For Shearing	21
2.4	Modeling of Trimming Operation	21
3.	THEORY AND FINITE ELEMENT FORMULATION	24
3.1	Steps of the Finite Element Analysis	24
3.2	Nonlinear Finite Element Analysis	25
3.3	Parameters Affecting the Metal Forming Simulations ...	25
3.4	Finite Element Types Used in Metal Forming	26
3.5	Failure Criteria	28
3.5.1	Shear Strain Energy Density	29
3.5.2	Effective Plastic Strain	29
3.5.3	Freudenthal Fracture Criterion	29
3.5.4	Cockroft-Latham Failure Criteria	30
3.5.5	Brozzo Criterion	31
3.5.6	Oyane Criterion	31
3.6	User-Subroutine	32
4.	VERIFICATION OF THE ELEMENT ELIMINATION METHOD	34
4.1	Finite Element Analysis of Simple Tension Test	34
4.2	Simple Tension Test at Elevated Temperatures	43
5.	CASE STUDY	45
5.1	Manufacturing of the Part	46
5.2	Finite Element Simulation of the Trimming Operation	55
5.2.1	The Model	55
5.3	Finite Element Analysis of Trimming	57

5.4 Finite Element Analysis of Trimming with Modified Die Set	62
5.5 Application of the New Design and Verification of the Analysis	66
6. DISCUSSION AND CONCLUSIONS	70
6.1 Conclusion	70
6.2 Future Work	70
7. REFERENCES	72

APPENDICES

A. Source Code of User-Subroutine	80
A.1 ELMVAR Utility Routine	84
A.2 Sample Output	85
B. Data and Results of Simple Tension Test at Room Temperature	88
B.1 Experimental Procedure	90
C. Tension Test Results of C45 Material Used In Chapter 5 ...	99
D. Technical Drawings of AKSAN 198-290.2 and Trimming Die Set	105
E. SPC Data	108
F. Properties of Hard-facing Electrode	113
G. Properties of Temperature Measuring Equipment	115

LIST OF FIGURES

FIGURE

3.1 Element 125 and layout of its integration points.....	27
3.2 Schematic drawing of Element 157.....	28
3.3 Algorithm of the subroutine. Main solver stands for the commercial FEA package.....	33
4.1 Finite Element Model of the Tensile Specimen	35
4.2 Finite Element Mesh in the Shearing Region.....	36
4.3 Stress-strain Graph Used in the Analysis.....	37
4.4 Stress Distribution at the Instant of Failure.....	38
4.5 Stress Distribution at the Failure Region.....	39
4.6 Equivalent Plastic Strain Distribution at the Instant of Failure	40
4.7 Plastic Strain Distribution at the Failure Region	41
4.8 Equivalent von Mises Stress vs Displacement Graph of the Failed Element.....	42
5.1 The part used in case study	45
5.2 Manufacturing steps of the forging 198-290.2.....	47
5.3 Heating of the part in the induction furnace (Step1).....	48
5.4a The heated part is placed into the upsetting die.	49
5.4b Upsetting (Step2).....	50
5.5 Part is elongated by forging in longitudinal axis (Step 3).....	50
5.6 After Step 3 the part is forty percent longer	51
5.7 Preform forging (Step 4 - 5).....	51
5.8 Final shape (Step 6).....	53
5.9 Inappropriate clearances caused jamming in trimming die	53
5.10 Trimming dies needed frequent maintenance	54

5.11 High wear rates in trimming dies increased down-time	54
5.12 3D model of trimming die	55
5.13 3D Finite element model of the workpiece	56
5.14 Finite element mesh is finer around the trimming region thick....	56
5.15 Top view of stress distribution of the workpiece in unmodified die	58
5.16 Perspective view of stress distribution of the workpiece in unmodified die.....	59
5.17 Plastic strain distribution of the workpiece in unmodified die	60
5.18 Plastic strain distribution of the workpiece in unmodified die	61
5.19 Modification in the trimming die	63
5.20 Model of workpiece in modified die	63
5.21 Plastic strain distribution of the workpiece in modified die.....	64
5.22 Plastic strain distribution of the workpiece in modified die	65
5.23 Side view of part with unacceptable flash residual.... ..	66
5.24 Closer view of the defective region	67
5.25 Schematic view of the application of die modification	68
5.26 Part which was produced with the improved trimming die design	68
5.27 No irregular cutting surface or flash residual in new design	69
5.28 The cutting surface without any defect.....	69

CHAPTER I

INTRODUCTION

Forging is one of the oldest manufacturing processes used to manufacture high strength metal products. Hot metal is shaped by impact forces taking the advantage of strain hardening. Blacksmiths used forging to produce high quality swords in the ancient times. Later, as the technology advanced forging is used to manufacture cannon and rifle parts in Europe. After the industrial revolution, use of this process spreaded quickly with the growing automobile industry and later extended to high technology areas such as aerospace industry because of its unique properties.

Forging is classified as cold, warm, and hot forging with respect to the temperature at which the part is formed. In hot forging raw material is generally formed in several steps. During this multi-step manufacturing operation excessive material forms the flash around the workpiece. Flash formation is an integrated part of forging and all forging operations produces flash except the net-shape precision forging. Altan and Vazquez showed in a recent study that, in conventional hot forging of connecting rods, the material wasted to the flash accounts approximately 20-40% of the original workpiece [1]. In order to reduce the cost of forged products, the forging must be performed in a closed cavity to obtain near-net or net shape parts. In flashless forging, the volume distribution of the preform must be accurately controlled to avoid overloading the dies and to fill the cavity. Additionally, the preform must be simple enough to be mass-produced. But generally the part to be forged is too complex for closed-die flashless forging, or the preform must be manufactured to very tight tolerances and in a complex shape to be able to obtain the desired forged shape. Because of all these problems it is

more feasible to forge parts in open dies with an acceptable amount of flash. In this case an additional die, the trimming die, should be manufactured.

As stated above trimming operation accompanies the manufacture of almost all forged parts. It is used not only in forging but also as a separate process in sheet metal forming. The process of trimming in flash removal dies resembles in many ways to the cutting operation in sheet metal forming. The process of separating adjacent parts of a sheet through controlled fracture cannot be described as either purely plastic deformation or as machining. It is basically a shearing operation.

Vazquez and Fujikawa investigated shearing phenomenon by using experimental and numerical methods [1, 2]. Recently, with the emergence of advanced engineering numerical analysis tools such as the finite element analysis (FEA), research has shifted from experimental to numerical fields. Having originated from the academic community, FEA found a wide application in industry with the help of advancing computer technology. In spite of the fact that commercial FEA packages are available in the market since 1980s, the technology still has some shortcomings and academic studies on certain extreme issues such as spring back, shearing, material failure and buckling continue. Most of the commercial packages are general purpose codes and their area of application in solid mechanics extends from simple linear static analysis to complex 3D coupled non-linear elastic-plastic analysis.

The use of these numerical tools has some advantages and disadvantages. Using an FEA program is getting easier than before and using them do not require specialized and highly trained analysts as before.

However, their prices are quite high for a small or mid-size manufacturing company. Also they are not still considered totally reliable by many users, and simulation results are generally needed to be verified by experiments or prototypes.

Shearing simulation has a wide area of application including fracture mechanics, metal cutting, blanking, and trimming. Different researchers use different failure criteria and various finite element algorithms are used to simulate this phenomenon. Most of the today's commercial FEA codes contain material failure modeling capability, however, they do not contain well established, ready to use shearing/trimming, and material failure simulation procedures. Generally additional user subroutines are necessary.

1.1 Survey of Previous Literature

Global competition requires that manufacturing industry utilizes practical and proven CAD, CAM and CAE techniques for rapid and cost effective process design and die manufacturing. Thus, numerical simulation of bulk metal forming processes is increasingly applied to eliminate forming defects, predict and optimize process variables, and to predict stresses in dies for preventing premature die failure [1, 3]. With the increasing competition, companies search ways for manufacturing parts faster and in better quality. Therefore the application of computer aided engineering and physical modeling techniques continue to increase in forging research and development studies. In using tools such as the finite element modeling and experiments with model materials, the forging tool designer can decrease costs by improving achievable tolerances, increasing tool life, predicting and preventing flow defects, and predicting part properties.

Since the late 1980s, the commercial based forging analysis software is in the market and they brought some benefits for optimizing forging processes. Several hot-forging examples made with the help of FEA simulations applied in the factory floor are available in the literature [2, 3]. Fujikawa used finite-element simulation to reduce the amount of input material for crankshaft forging. Also as a second example a die stress analysis for extending the lifetime of a die for forging side

flanges is given. And finally an application of CAE for the development of a forging expert system to prevent defects in hot-forged components is presented.

Examples of three-dimensional bulk forming modeling based on finite element method (FEM) are also available in literature [4]. Tin et al. reviewed the FEM formulations and discussed many considerations such as geometry representations, element selections, volume constancy, equation solvers and meshing methods. The updated Lagrangian method is employed in the FEM calculation, and an automated remeshing procedure is used to be able to continue the simulation when the mesh is severely distorted. To demonstrate the methodology presented, some successful applications of the program to various forming processes such as ingot breakdown, extrusion and orbital forging are presented.

Forging is used in manufacture of gears where possible because of the high production rate and because parts manufactured by forging is stronger than the parts manufactured by other methods. Therefore forming simulations are becoming common practice in gear manufacture. Bevel gear forging has several advantages as compared with conventional gear forming by a cutting process. For example, it reduces the material loss and the production lead-time and also has the advantage in product quality improvement of using plastic material flow in the gear teeth [5]. In general, gear forging has a process sequence including preforming and final forming because of the geometrical complexity of its tooth profile. Despite the importance of designing the process sequence, conventionally it has been done by the design expert with exhaustive trial-and-error. Recently, there have been many trial approaches to find the optimal process and die design, and to acquire the quality-related information after forming from simulation using the FEM. Vazquez stated that the bevel gear forging process could be simulated by three-dimensional FEM based on rigid-plastic material modeling, and it could be applied to the die design consideration to improve the product quality and to secure the effective material flow. Finite element simulations were performed for two types of bevel gear forging processes to find a defect-free forging process, and comparisons are made between

the two processes. It has been thus shown how an improvement can be made through an improved design using finite element simulation.

Commercial finite element codes are not adequate to simulate trimming. A considerable number of studies focus on shearing/trimming simulation and practical aspects of shearing. Breitling et al [6] describes the commonly used shearing equipment and summarizes the results of simulating the shearing process by means of a modified 2D Finite Element Method (FEM) code. All the necessary shear features required for high productivity are reviewed and a computerized system to control the volume of the sheared billets is described in detail. Several basic shearing simulations were performed. It was shown that the influence of process variables such as blade clearance, material properties and tooling configurations could be simulated with a good correlation to experimental results. Furthermore, the FEM simulation provides additional information about the necessary shearing force and the strain peaks within the sheared surface which may result in micro cracks.

1.1.1 Applications of Shearing Simulation in Manufacturing Operations

Application of shearing/trimming simulation in the manufacturing simulations is a new and rapidly growing area of research. Especially there is extensive amount of literature on the shearing simulation applications in metal cutting.

Modeling and simulation of cutting processes have the potential for improving cutting tool designs and selecting optimum conditions, especially in advanced applications such as high-speed milling. End milling of die/mold steels is a highly demanding operation because of the temperatures and stresses generated on the cutting tool due to high workpiece hardness. Özel and Rodriguez developed a methodology for simulating the cutting process in flat end milling operation [7, 8]. It was presented that chip flow, cutting forces, tool stresses and temperatures could be analyzed using finite element analysis. As an application, machining of P-20 mold steel at 30 HRC hardness using uncoated carbide tooling was investigated.

Lin et al. presented a coupled model of the thermo-elastic-plastic material under large deformation for orthogonal cutting is used [9]. A chip separation criterion based on the critical value of the strain energy density is introduced into the analytical model. A method of twin node processing and a concept of loading/unloading were also presented for chip formation. The flow stress was taken as a function of strain, strain rate and temperature in order to reflect realistic behavior in metal cutting. The cutting tool was incrementally advanced forward from an initial stage of tool-workpiece engagement to a steady state of chip formation. The finite difference method was adopted to determine the temperature distribution within the chip and tool, and a finite element method, which was based on the thermo-elastic-plastic large deformation model, was used to simulate the entire metal cutting process. Also, the chip geometry, residual stresses in the machined surface, temperature distributions within the chip and tool, and tool forces were obtained by simulation. It was found out that the chip separation criterion value based on the strain energy density is a material constant and is independent of uncut chip thickness.

Strenkowski described a finite element model of orthogonal metal cutting [10]. The paper introduced a new chip separation criterion based on the effective plastic strain in the workpiece. Several cutting parameters, such as elastic-plastic material properties of the workpiece and tool, friction along the tool rake face, and geometry of the cutting edge and workpiece are investigated. The model predicts chip geometry, residual stresses in the workpiece, and tool stresses and forces, without any reliance on empirical metal cutting data. The paper is a good example of the use of a chip separation criterion based on effective plastic strain, which is also used in this study, in metal cutting. The chip separation method is found to be essential in predicting chip geometry and residual stresses with the finite element method.

In another study about orthogonal metal cutting emphasis was given on analyzing the effect of important factors, such as plastic flow of the workpiece material, friction at the tool-workpiece interface, and wear of the tool, on the cutting

process [11]. To simulate separation of the chip from the workpiece, superposition of two nodes at each nodal location of a parting line of the initial mesh was imposed. According to the developed algorithm, the superimposed nodes were constrained to assume identical displacements, until approaching to a specified small distance from the tool tip. At that juncture, the displacement constraint was removed and separation of the nodes was allowed. To investigate the significance of the deformation of the workpiece material on the cutting process, elastic-perfectly plastic and elastic-plastic with isotropic strain hardening and strain rate sensitivity constitutive laws were used in the analysis. For simplicity, the tool material and the built-up edge were modeled as perfectly rigid. Spatial distributions of the equivalent total plastic strain and the von Mises equivalent stress corresponding to steady-state cutting conditions and the normal and shear stresses at the rake face were investigated and results were interpreted qualitatively in terms of critical parameters. The influence of interfacial friction, metal flow characteristics, and wear at the rake face of the tool on the steady-state magnitudes of the cutting forces, shear plane angle, chip thickness, and chip-tool contact length were also investigated.

Park and Dornfeld presented a finite element model of orthogonal metal cutting including burr formation [12]. A metal-cutting simulation procedure based on a ductile failure criterion was proposed for the purpose of better understanding the burr formation mechanism and obtaining a quantitative analysis of burrs using the finite element method. Four stages of burr formation, i.e., initiation, initial development, pivoting point, and final development stages, were investigated based on the stress and strain contours with the progressive change of geometry at the edge of the work piece.

Lo et al. investigated the formation of discontinuous chip using finite element method [13]. The cutting simulation was conducted on 60-40 brass (60% Cu, 40% Zn) under an extremely low cutting speed. The region of the maximum strain energy density (SED) distribution value relative to the minimum value was used as the criterion to predict the initial breakage location under the assumption that the curvature direction of the maximum SED was the

direction of crack growth. The shape and cutting force of discontinuous chip crack, the stress and strain distribution of the workpiece and chip, and the variation of various nodal forces on the chip-tool interface were derived.

Metal cutting operations are extensively investigated using computational methods. However, studies on other manufacturing operations involving shearing and material separation are still very limited and this area of research promises great improvements. Especially in flash removal operations in forging finite element analysis can be used effectively to improve the process parameters.

1.1.2 Failure Criteria Used in Shearing Analysis

There are several failure criteria commonly used in FEA simulations. Most commonly used are Cockroft-Latham, McClintock, Freudenthal, Brozzo, shear strain energy density, effective plastic strain, plastic work per unit volume. The first four of these criteria are investigated in [14] extensively.

Goieva described the utilization of ductile fracture criteria in conjunction with the FEM for predicting failures in cold bulk metal forming [14]. Four fracture criteria, i.e. Cockroft-Latham, McClintock, Freudenthal, and Brozzo, were selected and their relative accuracy for predicting and quantifying fracture initiation sites were investigated. Experiments with ring, cylindrical, tapered, and flanged upset samples were used in the investigation. The implementation of ductile fracture criteria into a rigid-plastic finite element computer program was presented. Only two of the criteria, Cockroft-Latham and McClintock criterion, predicted correctly the location of fracture initiation.

Cockroft and Latham criterion was also used in [15]. In this study the limitation and applicability of the ductile fracture were investigated. For this purpose, experimental and numerical investigations for simple upsetting were conducted for different aluminum alloys. As a result, the fracture mode of each

alloy was observed. Based on experimental data of simple upsetting, the damage factors for the same two criteria were calculated by adopting rigid-viscoplastic finite element analysis. With this approach, the prediction of surface cracking was attempted by comparing the calculated limiting damage factors between simple upsetting and pin-shape forging.

Cold forging process were analyzed by MacCormack [16] in which a hexagonal shape on the head of a fastener were trimmed. The fastener head geometry is achieved by forcing the die, called the trim die, onto the workpiece, where a combined forging and cutting action produced the desired well-known hexagonal shape for the head. The trim die material was taken as M2 high-speed steel. A finite element analysis package implemented to simulate the trim die forging process utilized Cockroft and Latham's fracture criterion to calculate the damage induced within the workpiece material during the process. Elements are deleted from the model when they exceeded a specified damage value. The trim die geometry, if incorrect, can cause premature shearing of the waste material during forging. This premature shearing has a negative effect on tool life and the forging machinery. In the study the relationship between the trim die geometry and its final stopping distance, the consequent induced stresses and the energy required to shear off this excess material was investigated. Finally the effect of altering the damage value C , which is used in the Cockroft-Latham failure criterion, was analyzed. From such investigations, conclusions as the optimum trim die shape and final stopping distance, which would facilitate increased die life, can be obtained.

Several researchers investigated elasto-plastic deformations with applications to metal forming and impact using numerical and experimental procedures. In a study by Creus et al. the procedure for the integration of stresses that may give rise to numerical instabilities and propose a solution were investigated [17]. Also, some initial results on work with coupled effects of temperature, plasticity and damage were presented.

Peric is concerned with adaptive strategies for finite element simulation of large deformations of elasto-plastic solids at finite strains [18]. Computational issues relevant for application of adaptive strategies to solution of industrial problems were particularly discussed. The need for a rigorous treatment of both theoretical and algorithmic issues was emphasized and aspects important to the solution of practical problems were discussed. Some possibilities for the choice of error indicators were presented. Detailed analysis was also given to the transfer of variables between moving meshes for history-dependent elasto-plastic materials in the presence of large strains. A set of numerical examples representing a wide range of industrial problems was provided to illustrate the effectiveness and robustness of the developed approach. The application areas covered include metal forming with thermo-mechanical coupling, high-speed machining and blanking, and projectile impact modeling.

Studies that use the finite-element technique to predict fracture initiation in a range of simple metal forming operations are also available in literature. These studies cover typical processes and enables deformation and fracture initiation to be examined under several different loading conditions. Three types of metal forming operation were considered, simple upsetting, axi-symmetric extrusion, and strip compression and tension in [19]. Using a program developed to deal with metal forming analysis, the local stress and strain distributions were determined. These values were then used with previously published continuum fracture criteria to predict fracture initiation sites. The predictions so obtained were subsequently compared with experimental observations. Only one criterion had successfully predicted the fracture initiation site found experimentally in all the operations examined in this paper: that of a critical value of generalized plastic work per unit volume. This criterion was also used to predict the level of experimental deformation at which fracture should occur, but only with partial success.

In the study presented by Lee and Joun, an application-oriented piercing simulation technique in automatic forging simulation by the rigid-viscoplastic finite element method was explained [20]. In that approach, it was assumed that

fracture in piercing takes place at the instant when the maximum accumulated damage around the shearing region reaches the critical damage value of the material. Separation was made along the line connecting the two die edges. A method of obtaining the critical damage value by comparing the tensile test result with that of the analysis was given, with emphasis on the effect of the strain hardening exponent on the critical damage value. The approach presented was verified by a test piercing process with a medium-carbon steel and was applied successfully to the automatic simulation of a sequence of six-stage compound forging processes.

Studies to develop an accurate finite element model valid for the numerical description of processes such as sheet-metal cutting processes by material shearing mechanisms had been conducted by several researchers [21, 22]. Damage and crack propagation had been taken into account by means of an elasto-plastic constitutive law. To study the effects of variation of process parameters on the geometry of sheared edges and the force-punch penetration evolution, the algorithm of calculation by means of user routine (UMAT) of ABAQUS/Standard finite element code were implemented. Final results of the FEM simulation were reported to agree with the experimental ones.

Results of another simulation of the blanking process by means of a modified FEM code can be found in [23]. Several modifications were made to the commercially available code DEFORM in order to simulate the material fracture. Unlike most other approaches, it was possible to obtain each of the zones of a blanked part edge such as roll over, shear zone, rupture zone and burr. Several blanking simulations were performed and the results were compared with experimental studies. It was shown that the influence of process variables such as punch-die clearance, material properties and punch and die wear could be simulated with a good correlation to experimental results. Furthermore, it was shown in this study that the simulated and experimentally obtained load stroke curves show the same changes of shape and absolute value due to variations in process conditions.

1.1.3 Influence of Input Variables on the Trimming Operation

Attaining high quality input data for the finite element analysis of forging could be difficult and expensive. The sensitivity of the results of an FEA of forging to key input parameters were investigated by several researchers [24]. The case examined in Snape [24] was a closed-die forging operation. Six input parameters, four used to define the plastic flow stress of the workpiece and two to define the conditions at the die-workpiece boundary, were varied. Results of full-factorial experiments, with each of the variable parameters assigned nine different values, were compared and analyzed. Each response was then subjected to a regression analysis to establish linearity. In this way it was possible to assess the accuracy required of input data relative to the output requirements of the analysis. In the constitutive equation used for flow stress, the constant coefficient and temperature sensitivity term had a greater influence on the FEA results than that the strain-rate sensitivity and strain-hardening terms. At the die-workpiece interface, friction was found to be more important than the cooling effect of the die.

Process parameters affecting the trimming process can be determined in various ways. One of them is using in-die sensors. The performance of in-die sensors for controlling the stamping process are discussed by Breitling [25]. Piezo based as well as strain gage based in-die sensors were mounted at different locations within a progressive die. Furthermore, these signals were compared with load curves of press frame mounted sensors and the acoustic emission acquired from a triaxial acceleration sensor. The signals acquired from the different in-die sensors at the different mounting locations showed all the different phases of the process. It was shown that changing process variables such as punch-die clearance, material properties, stroke rate and punch-die alignment results in different load-stroke curves.

However, this is not always the best way for determining process parameters in metal forming. Some parameters can only be obtained by computer simulations and cannot be directly measured.

The clearance between the punch and the die plays an important role in the trimming and shearing processes. The selection of the clearance will influence the life of the die or punch, the blanking force, the unloading force and the dimensional precision. In several publications the punch—die clearance values for a given sheet material and thickness are optimized, using the finite element technique and Cockroft and Latham fracture criterion [26].

Several other studies using commercial FEA software are done by researchers to obtain optimum process parameters. Shugin investigated that [27], the cutting force curves and the cutting surface parameters which can be used to describe the quality of the blankings were measured for various clearance values. Simulation was accomplished by MARC Autoforge.

Faura et al. showed a similar methodology to obtain optimum punch-die clearance values for a given sheet material and thickness to be blanked was proposed. ANSYS was used with the fracture criterion Cockroft and Latham.

Elastic-plastic finite element method based on the incremental theory of plasticity is commonly used in sheet metal analyses. The blank diameters are considered in various ranges [29]. These studies has helped to evaluate the influence of tool clearance, friction, sheet thickness, punch/die size and blanking layout on the sheet deformation. The punch load variation with tool travel and stress distribution in the sheet had been obtained. The results indicate that a reduction in the tool clearance increases the blanking load. The blanking load increases with an increase in the coefficient of friction. These observations are reported to be very similar to the case of blanking of larger size components. Further, these effects are very similar in the case of both single and double blanking. The results of these studies have showed that an interblanking site distance of about twice the sheet

thickness is good to reduce the thinning of sheet at the intermediate regions between the two blanking sites. For a particular sheet thickness, the blanking load requirement reduces as the blank diameter increases [29].

1.1.4 Finite Element Simulation

There are several algorithms commonly used in the simulation of shearing in the finite element method. Currently there are two methods that are commonly adopted by the researchers. These are element elimination and node separation methods. Both methods are referred in numerous publications. Node separation is more recent and a more complex method.

Node separation method is one of the subjects being extensively investigated by many researchers. A newly developed computer program, based on a conventional computer program of the finite-element method, with which the behavior of crack growth after ductile fracture can be analyzed, is presented by Komori [33]. The phenomenon that a material is divided into two parts upon shearing has been simulated by node separation, and the following results were obtained. First, in order to perform a precise simulation, a method for representing the sharp change in the direction of material flow at the tool corners was introduced. In this method tool displacement is controlled such that an element is fractured in each step. Secondly, analytical results of the shape of the sheared surface, the length of the sheared surface, the length of the fractured surface and the relationship between the punch displacement and punch force were found to agree with the experimental results [33].

Element elimination is another method of modeling shearing. In element elimination method elements in the finite element mesh are “deleted” from the mesh in case they satisfy certain predetermined conditions. One drawback of this method is that, some of the volume and mass of the initial workpiece is lost due to the deleted elements. Therefore the mesh around the possible failure region should

be very fine in order to minimize the lost mass. Element elimination method is used in some popular FEA codes such as DEFORM.

There are also other methods that are used in cooperation with the element elimination and node separation methods which help to determine the point of failure. Fracture mechanics analysis and forming limit diagrams are two of these methods.

The area of the true stress/strain diagram determined under tensile test conditions is equal to the energy absorbed per unit volume at the point of fracture. This energy value can be used in simulation of shearing. In the case of tensile as well as other loading tests like compression, low cycle fatigue, etc. a spreading crack will be initiated when the critical specific fracture energy characteristic of the material has been absorbed whereby the proportionality law of notched specimens can then be derived. The specific fracture energy of notched tensile test specimens as expressed in the function of temperature describes the brittle fracture sensitivity of the material. From the specific fracture energy of notched specimens the fracture toughness and the critical energy release rate can be determined. The method described above is also adaptable for the determination of the brittle fracture sensitivity of welded joints [34]. It is shown in this study that, this data can be used to determine fracture initiation sites in shearing simulations.

Forming limit diagrams (FLD's) in connection with calibrated FEM simulations can serve as a powerful aid towards the prediction of cracks in sheet metal forming. In Xu and Weinmann's study [35] a method is proposed to develop forming limits for aluminum using Hill's 1948 and 1993 yield criteria. These criteria are compared with experimental data for Aluminum 6111-T4. It is found that Hill's 1993 yield criterion can characterize localized necking in aluminum sheets well, while Hill's 1948 criterion cannot.

1.2 Scope of This Study

Primary goal of this study is to successfully model the shearing operation by using the finite element method. In modeling a commercial code will be used to analyze the shearing operation in practical engineering problems. However, most of the commercial analysis packages cannot model material failure or fracture. Hence, a user subroutine will be developed.

The other primary goal of this study is to solve problems that arise in trimming dies used in forging industry with the help of the simulation methods developed. Following problems in trimming dies that are not designed properly arise because of the dies and process parameters and lack of experience in the manufacturing:

- Excessive burr formation around the cutting surface
- Irregular residuals of burr formation around the bottom surface after the cutting operation
- Irregular cut surface
- Die and punch jamming due to the inappropriate clearance values
- Premature die failure due to high wear rates

It is intended to modify trimming dies with the help of the data obtained in the finite element simulations to solve the problems addressed above.

Survey of literature reveals that modeling of shearing and determination of failure are currently being investigated by many researchers. There is also considerable amount of literature on die optimization. However, in very few studies these are combined to solve real life engineering problems. In this thesis study, two failure criteria will be implemented by a user-subroutine developed for a commercial finite element code to analyze the trimming process.

Chapter 1 covers previous literature reviewed on forging, trimming, and finite element method. Chapter 2 focuses on mechanics of and parameters affecting the trimming process. Chapter 3 reviews the parameters of the finite element analysis used, failure criteria in the finite element simulations and finite element algorithms used in modeling the shearing phenomenon. This chapter later presents the user-subroutine developed. Verification of the accuracy of the finite element simulation and the user-subroutine developed is presented in Chapter 5. Chapter 6 presents the case study done to solve addressed problems in flash trimming dies used in forging industry.



CHAPTER II

TRIMMING PROCESS

2.1 Trimming Operation

Trimming is the mechanical cutting of materials without formation of chips and used commonly in forging, casting, and sheet metal forming to obtain the desired shape or to remove flash. The metal is subjected to both tensile and compressive stresses. Stretching beyond the elastic limit takes place, plastic deformation occurs and finally fracturing starts through cleavage planes in the reduced area which results with shearing.

There are several effective parameters in the trimming process. Most important ones are tool clearance, friction, sheet thickness, punch/die size, and blanking layout on the sheet [38, 39].

Many commercial FEA programs contain crack initiation and propagation simulation options, which may be used in cutting and shearing simulations. However, this procedure [40, 44] is complicated and not effective in almost all commercial codes.

Accumulated damage, strain energy density distribution, the critical value of generalized plastic work per unit volume and several other damage criteria are applied to model shearing process [45, 47]. These criteria can be utilized to determine the material failure by using different techniques such as element elimination and node separation methods [48]. In this study finite element analysis of shearing process by element elimination method with the use of two different stress criteria are presented.

2.2 Mechanics of Shearing

The process of trimming in flash removal dies resembles in many ways to the blanking operation in sheet metal. On penetration of the tool edges, the sheet is first pushed into the die, and plastic deformation results in a rounding of the edge of the blank. Because the clearance between the two tools is only 5% to 10% of the thickness of the metal being cut for sheet metal, the deformation is highly localized. The blank is pushed into the die by extrusion-like plastic deformation, which is characterized by steadily increasing forces. After some critical deformation, cracks are generated at a slight angle to the cutting direction, initially at the die edge. When the penetration reaches about 15% to 60% of the thickness of the metal, the amount depending upon the ductility and strength, the applied stress exceeds the shear strength and the metal suddenly shears or ruptures through the remainder of its thickness. As the cracks meet, the cutting force drops even though the cutting edges had moved only partly through the thickness of the sheet.

The condition and alignment of the punch and the shearing blades, and the clearance between them has influence on the quality of the sheared edges. If blank holder is used, its pressure is also an important parameter in shearing.

Because of the normal non-homogeneities in a metal and the possibility of non-uniform clearance between the shear blades, the final shearing may not occur uniformly. Failure of the material starts at the weakest points and proceed progressively and intermittently to the next stronger locations. With a very tight clearance, the cracks miss each other and the cut is then completed by a secondary tearing process. This produces a notched edge roughly midway in the sheet thickness. On the other hand, excessive clearance allows extensive plastic deformation. The separation is delayed and a long burr is pulled out at the upper edge.

The tool edges wear and become rounded as thousands of parts are being cut. Then burr forms even with an optimum clearance. The jagged edge of the burr with sharp roots acts like a stress concentrator and reduces the useful operation life of the part. The selection of the optimum clearance is crucial in the operation. A small clearance leads to more rapid tool wear. Therefore the clearance should be chosen as large as permissible.

2.3 Factors Affecting Shearing

2.3.1 Clearance

Clearance is the measured space between the mating members of a die set. In shearing/trimming operation clearance is one of the most important criteria. Proper clearance between the cutting edges enables the fractures to meet and the fractured portion of the sheared edge has a smooth appearance. However, the load on the punch is almost independent of the clearance. Experimental clearance ranges for commonly used materials are given in the Table 2.1.

TABLE 2.1 Experimental clearance values for common materials [38]

Material	Hardness	Clearance (% of material thickness)
Mild Steel	94 – 144	5 – 10
70/30 Brass	77 – 110	0 – 10
Copper	64 – 93	0 – 10
Zinc	61	0 – 5
Aluminum	21 – 28	0 – 5

Angular clearance, on the other hand, is necessary for the blank or the slug to clear the die. Angular clearance per side changes from 0.25 to 2.0 .

2.3.2 Force Required For Shearing

Then the shearing force (F_s) is calculated as

$$F_s = C_1 \sigma_u h l \quad (2.1)$$

where σ_u the ultimate tensile stress, h is the sheet thickness, l is the length of the cut, C_1 is a constant that is 0.85 for ductile materials and about 0.7 for less ductile ones [49].

Parallel shearing edges can lead to very high forces, which can then be reduced by placing the two shearing edges at an angle to each other. In that case only the instantaneously sheared length needs to be considered.

2.4 Modeling of Trimming Operation

Die or tool design and manufacturing, and interactions between the workpiece material and the dies are the key issues, while dimensional tolerances, surface finish, and structural integrity of the final part are the key goals throughout the forming process.

In designing and developing bulk metal forming processes, important parameters are workpiece material (shape and size, chemical composition and microstructure, flow properties under processing conditions, thermal and physical properties), dies and tools (geometry, surface conditions, material and hardness, surface coating, temperature, stiffness and accuracy), interface conditions (surface finish, lubrication, friction, heat transfer), workzone (mechanics of plastic deformation, material flow, stresses, velocities, temperatures), and equipment used (speed, production rate, force and energy capabilities, rigidity and accuracy). Understanding effects of these parameters allow the prediction of the characteristics of the formed product as well as the criteria to be considered in the die design.

In die design for metal forming operations, process modeling is used to predict metal flow, stress and temperature distributions, stresses and forces applied on tools, and potential sources of defects and failures. In some cases it's even possible to predict elastic recovery and residual stresses. Application of 2D simulations, e.g., axi-symmetric, plane strain and plane stress are widely used in research. Manufacturing companies still rely on the past experiences in tool and die design and the use of numerical methods is not still a common practice.

Computer integrated product and process design for metal forming consists of the following steps:

- 1) Preparation of a preliminary die design and selection of process parameters by using experience knowledge and empirical formulas.
- 2) Verification of preliminary design and process conditions using process modeling. This step is completed with the help of the CAD/CAM CAE software including the finite element method
- 3) Modification of die design and initial selection of process variables based on the simulation results
- 4) Complete die design and manufacture of dies
- 5) Die try-outs on production equipment
- 6) Modification of die design and process conditions if necessary to produce good quality parts.

Practical applications of mechanical process simulation in metal forming include:

- 1) Design of forging sequences in cold and hot forging, including the prediction of forming forces, die stresses, and preform shapes. This step will help the proper selection of forging equipment. Tooling and dies will be prepared according to the process requirements.

- 2) Prediction and optimization of flash dimensions in hot forging. Use of simulations will reduce flash and scrap material and therefore a considerable gain in material cost will be obtained.
- 3) Prediction of die stresses, fracture and die wear improvements in process variables and die design to reduce die failure. With the help of the stress analysis die shape may be optimized for best stress distribution which in turn increases die life. With the help of this kind of simulations die life can be extended 6-8 folds [49].
- 4) Prediction and elimination of failures, surface folds or fractures as well as internal fractures. This will improve the workpiece quality and improve die life.
- 5) Investigation of the effects of friction upon metal flow. Parts of the die experiencing high friction will wear out fast. These sections may be reinforced during die manufacture.
- 7) Investigation of metal flow in multiple action forging and selection of various tool motions and sequences. Forming sequence will be selected for best quality and minimum flash.
- 8) Prediction of microstructure and properties, elastic recoveries and residual stresses. Dies may be designed to prevent or minimize the spring back or other undesirable effects.

Finite element method is an important tool in the analysis of metal forming operations. It is also applied in trimming and shearing processes. In this study the trimming process is analyzed by a commercial finite element code together with the element elimination algorithm developed.

CHAPTER III

THEORY AND FINITE ELEMENT FORMULATION

The commercial FEA package, MSC.MARC/Mentat 2001 [60], is used in this study. The formulation is based on the virtual work principle and an elastic-plastic updated Lagrangian formulation.

3.1 Steps of the Finite Element Analysis

To be able to successfully apply the finite element method to the metal forming operations the following requirements should be fulfilled:

1. The physical problem should be well-defined for the application of simulation.
2. The idealization of this physical problem should be done correctly: Simplifications and assumptions should be reasonable. Unnecessary details should be eliminated.
3. The idealized problem should have the correct spatial discretization: Type of elements used, topology of element mesh, and the density of element mesh should be constructed according to the nature of the problem.
4. Boundary conditions of the physical model should be investigated and applied in the simulation: friction, heat transfer, machines, dies, etc.
5. Correct material laws and parameters should be used in the simulation: flow curve, anisotropy, failure, etc.
6. Numerical parameters used in the simulation should be chosen accordingly: penalty factors, convergence limits, increment sizes, remeshing criterion, etc.

7. The simulation should be “economical”: Computation times and the time required to prepare the model should be reasonable, storage requirements of the model and the results should also be within the physical limits.
8. The results should be evaluated carefully and checked whether they are reasonable or not.

3.2 Nonlinear Finite Element Analysis

A problem is nonlinear if the force-displacement relationship depends on the current state (that is, current displacement, force, and stress-strain relations). There are three sources of nonlinearity:

1. Material nonlinearity
2. Geometric nonlinearity
3. Nonlinearity due to boundary conditions.

In material nonlinearity relationship between stresses and strains is nonlinear and observed in elastic-plastic analysis, elasto-viscoplasticity, creep etc. Geometric nonlinearity is the nonlinear relationship between strains and displacements, and nonlinear relation between stresses and forces. The third type of nonlinearity is non-linear boundary conditions and/or loads due to contact and friction.

3.3 Finite Element Formulations

There are two fundamental approaches in the finite element method. These are Lagrangian and Eulerian formulations. Eulerian formulation is generally used in fluid mechanics applications. In solid mechanics, Lagrangian meshes are widely used because it is possible to handle complicated boundaries and follow material points, so that history dependent materials can be treated accurately.

The Lagrangian formulation has two types: total Lagrangian formulation and updated Lagrange formulation. In this study updated Lagrange formulation has been used.

In the updated Lagrangian approach the derivatives and integrals in calculating the stress and strain values are taken with respect to the spatial (Eulerian) coordinates. The current configuration acts as the reference state. It is used in situations where rotations are large so that the nonlinear terms in the curvature expressions may no longer be neglected. Updated Lagrangian approach performs well in large strain plasticity analysis, and for calculations in which the plastic deformations cannot be assumed to be infinitesimal.

3.4 Finite Element Types Used in the Analysis

Simulations are run with several different element types in this study. 2D tensile test simulations are performed using ELEMENT 125 from the element library of MSC.MARC/Mentat 2001 because this element is suitable for large strain and shear analysis.

This is a second-order iso-parametric two-dimensional plane strain triangular element. Displacement and position (coordinates) within the element are interpolated from six sets of nodal values, the three corners and the three mid-sides (Figure 3.1). The interpolation function used in the element is such that each edge has parabolic variation along itself. This allows an accurate representation of the strain field in elastic analyses [59].

The stiffness of this element is formed using three-point integration. This element is suitable for all constitutive relations.

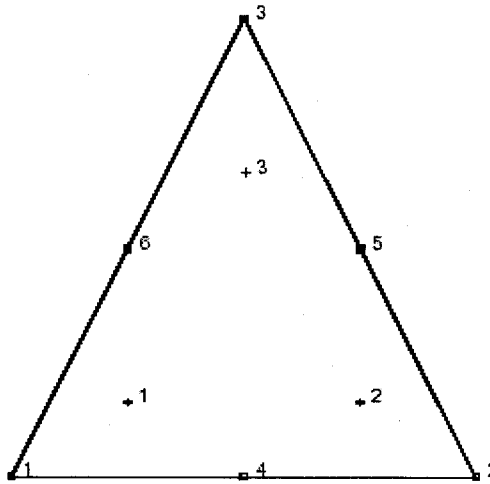


Figure 3.1 Element 125 and layout of its integration points

This element can be used in both total and updated Lagrange formulations. These properties are especially useful for successful simulation of shearing.

3D simulations are performed using ELEMENT 157 which is a three-dimensional, iso-parametric, 4+1-node, low-order, tetrahedron using Hermann formulation and with an additional pressure degree of freedom at each of the four corner nodes (Figure 3.3). It is written for incompressible or nearly incompressible three-dimensional applications. The shape function for the center node is a bubble function. Therefore, the displacements and the coordinates for the element are linearly distributed along the element boundaries. The stiffness of this element is formed using four Gaussian integration points. The degrees of freedom of the center node are condensed out on the element level before the assembly of the global matrix.

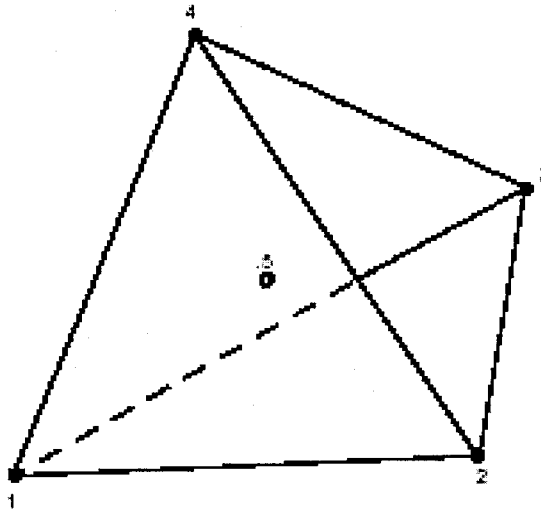


Figure 3.2 Schematic drawing of Element 157

This element can be used for incompressible elasticity via total Lagrangian formulations or for rubber elasticity and elasto-plasticity via updated Lagrangian formulations. Four integration points are used to correctly interpolate the cubic shape function. Five nodes per element (Figure 3.2) are used. Stresses and Strains are output at each integration point. For the case of large deformations, the stresses are the second Piola-Kirchhoff stresses and the strains are the Green strains.

3.5 Failure Criteria

Workability depends on the local conditions of stress, strain, strain rate, temperature and also on material factors, such as the resistance of a metal to failure. Failure in bulk metal forming usually occurs as ductile fracture, rarely as brittle fracture. Typical criteria for room-temperature ductile fracture are usually based on combinations of stress with strain or strain rate rather than on either of these quantities separately.

3.5.1 Shear Strain Energy Density

In the shear strain energy density the material is assumed to fail when the equivalent von Mises stress in the part is equal to the ultimate tensile strength of the material [52].

$$(\sigma_{xx} - \sigma_{yy})^2 + (\sigma_{yy} - \sigma_{zz})^2 + (\sigma_{zz} - \sigma_{xx})^2 + 6(\sigma_{xy}^2 + \sigma_{yz}^2 + \sigma_{zx}^2) = 2Y^2 \quad (3.1)$$

where σ_{ij} is the Cauchy stress tensor and Y is the yield stress.

3.5.2 Effective Plastic Strain

In the effective plastic strain energy failure criteria the material fails when the plastic strain reaches to the effective plastic strain. The effective plastic strain is obtained when the part is stressed up to the ultimate tensile strength. There are several advantages of using effective plastic strain as the failure criterion instead of the equivalent von Mises stress. Firstly at the instant just prior to the failure the equivalent plastic strain values around the failure point increases and a point of concentration, at which the failure criterion can be applied, is obtained. Area of maximum equivalent stress is much bigger compared to the area of equivalent plastic strain. Therefore, a narrow concentration region cannot be obtained with the equivalent von Mises stress criterion only. This makes the use of equivalent plastic strain value more feasible to use in shearing analyses.

3.5.3 Freudenthal Fracture Criterion

One of the earliest attempts to predict the point of failure was made by Freudenthal, introducing a critical value, C_1 , of the generalized plastic work per unit of volume at fracture [53],

$$\int_0^{\bar{\epsilon}^f} \sigma d\bar{\epsilon} = C_1 \quad (3.2)$$

where C_1 is determined as

$$C_1 = B \left(\frac{2}{\sqrt{3}} \right)^{n+1} (\sqrt{\alpha^2 + \alpha + 1})^{n+1} \varepsilon_z^n \Delta \varepsilon_z \quad (3.3)$$

In the above equation B is the material constant for the stress-strain curve of the material,

$$\sigma = B \bar{\varepsilon}^n \quad (3.4)$$

3.5.4. Cockcroft-Latham Failure Criteria

Starting from the importance of the largest tensile stress, M. G. Cockcroft and D. J. Latham developed a failure criterion to determine the workability of metals in 1968. This criterion is one of the earliest yet most widely accepted one. This fracture criterion is based on the critical value of the tensile strain energy per unit of volume. In other words:

$$\int_0^{\bar{\varepsilon}_f} \sigma_1 d\varepsilon = C_2 \quad (3.5)$$

This criterion is not based on a micro mechanical model of fracture. It determines the failure according to the dependence of the critical value at the fracture (C_2) to the level of the largest principal stress (σ_1) [53].

The experimental critical values at fracture for the Cockcroft-Latham criterion are obtained from:

$$C_2 = -\frac{B}{\sqrt{3}} \left(\frac{2}{\sqrt{3}} \right)^{n+1} (2\alpha + 1) (\sqrt{\alpha^2 + \alpha + 1})^n \varepsilon_z^n \Delta \varepsilon_z \quad (3.6)$$

3.5.5 Brozzo Criterion

For a given material at certain temperature and strain rate conditions, workability is also dependent on the level of the hydrostatic stress (σ_m). It is an experimentally verified fact that materials with limited formability can be deformed under high hydrostatic pressures. Brozzo criterion used the dependence of the workability to the level of both the largest principal stress (σ_1) and the hydrostatic stress (σ_m) [54, 55]. This criterion is actually an empirical modification of Cockcroft-Latham criterion:

$$\int_0^{\bar{\varepsilon}_f} \frac{2\sigma_1}{3(\sigma_1 - \sigma_m)} d\bar{\varepsilon} = C_3 \quad (3.7)$$

where the experimental critical values at fracture for the Brozzo criterion are:

$$C_3 = \frac{4}{3\sqrt{3}} \left(\frac{2\alpha + 1}{\alpha} \right) (\sqrt{\alpha^2 + \alpha + 1}) \Delta\varepsilon_z \quad (3.8)$$

3.5.6. Oyane Criterion

According to the basics of fracture mechanics, ductile fracture in bulk metal forming processes follows a void growth model. Due to this model, voids initiate at inclusions or hard second phase particles. These voids initiate generally in regions of the microstructure that are highly deformed. They grow under plastic deformation caused by normal or shear stress systems and finally link up between each other to form macroscopic cracks. Based on this model, Oyane derived a failure criteria based on the fundamental issues of the theory of plasticity for porous materials:

$$\int_0^{\bar{\varepsilon}_f} \left(1 + A \frac{\sigma_m}{\sigma} \right) d\bar{\varepsilon} = C_4 \quad (3.9)$$

In the above equation A is a material constant, which is determined experimentally, and C_4 is a material constant [54-58].

The experimental critical values at fracture for the Oyane criterion are:

$$C_4 = \frac{-\sqrt{3}(\sqrt{\alpha^2 + \alpha + 1}) + A(\alpha + 1)}{\sqrt{3}} \frac{2}{\sqrt{3}} \Delta \varepsilon_z \quad (3.10)$$

Experimental and theoretical comparisons of these criteria using FEA codes are available in literature [54].

3.6 User-Subroutine for Failure Analysis

In this study the subroutine is used with 2D plane strain triangular, 2D plane strain rectangular and 3D tetrahedral elements. Two different failure criteria, i.e. shear strain energy density and effective plastic strain are used. In all cases the user-subroutine was modified easily to change criteria used and returned consistent and accurate results. Source code of the subroutine is given in Appendix A.

The algorithm of the subroutine is given in Figure 3.3. The main solver, MARC, computes stress and strain values at each integration point of every element at each increment. This data is used as an input to the user-subroutine by a built-in subroutine, UACTIVE. This element data is compared with the maximum stress or strain value which is entered by the user in the subroutine. If the element data for the specific increment is greater than the critical, i.e. maximum stress or strain value the element is removed. A deactivated element does not contribute to the load, mass, stiffness, or internal force calculation. The subroutine is implemented into an element loop. An element loop means that the solver calls the subroutine at the beginning of every increment for each individual element.

The direct profile solver with bandwidth optimization was preferred as the solver. Direct methods are usually reliable, in that they give accurate results for virtually all problems at a predictable cost. The problem with these direct methods is that a large amount of memory (or disk space) is required, and the computational costs become very large [60]. In the particular case solution times were considerably high, but results were accurate.

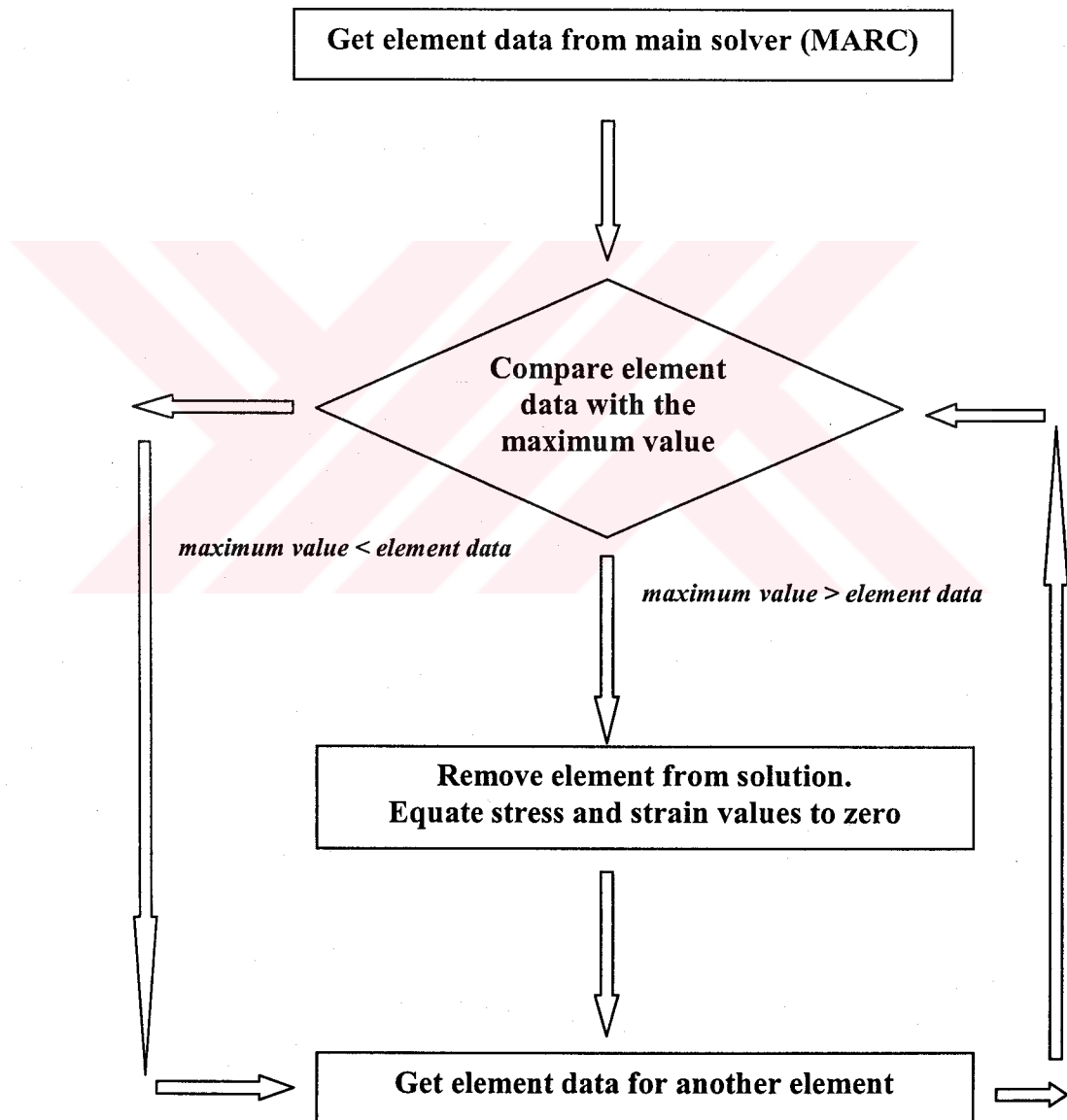


Figure 3.3 Algorithm of the subroutine. Main solver stands for the commercial FEA package

CHAPTER IV

VERIFICATION OF THE ELEMENT ELIMINATION METHOD

Simple tension test at room temperature and at elevated temperatures are done to verify simulation results and determine material properties, respectively. Experimental procedures, data obtained, measuring techniques and devices, and test apparatus with brief explanations are given in this section.

4.1 Finite Element Analysis of Simple Tension Test

Simple tension test at room temperature is analyzed to verify the simulation results with the experimental data. In the analysis a two-dimensional model consisting of 4878 elements is used. Half of the part is modeled and symmetry boundary condition is assigned along the longitudinal axis of the part (Figure 4.1). Mesh density is increased in the middle, where the material failure is expected. To ensure uniformity of the mesh distribution throughout the model half of the model is meshed and mirror image of the half is taken to form the final model (Figure 4.2). To model the simple tension test the nodes at the right hand side edge are displaced and zero displacement boundary conditions are assigned to the nodes at the left hand side edge.

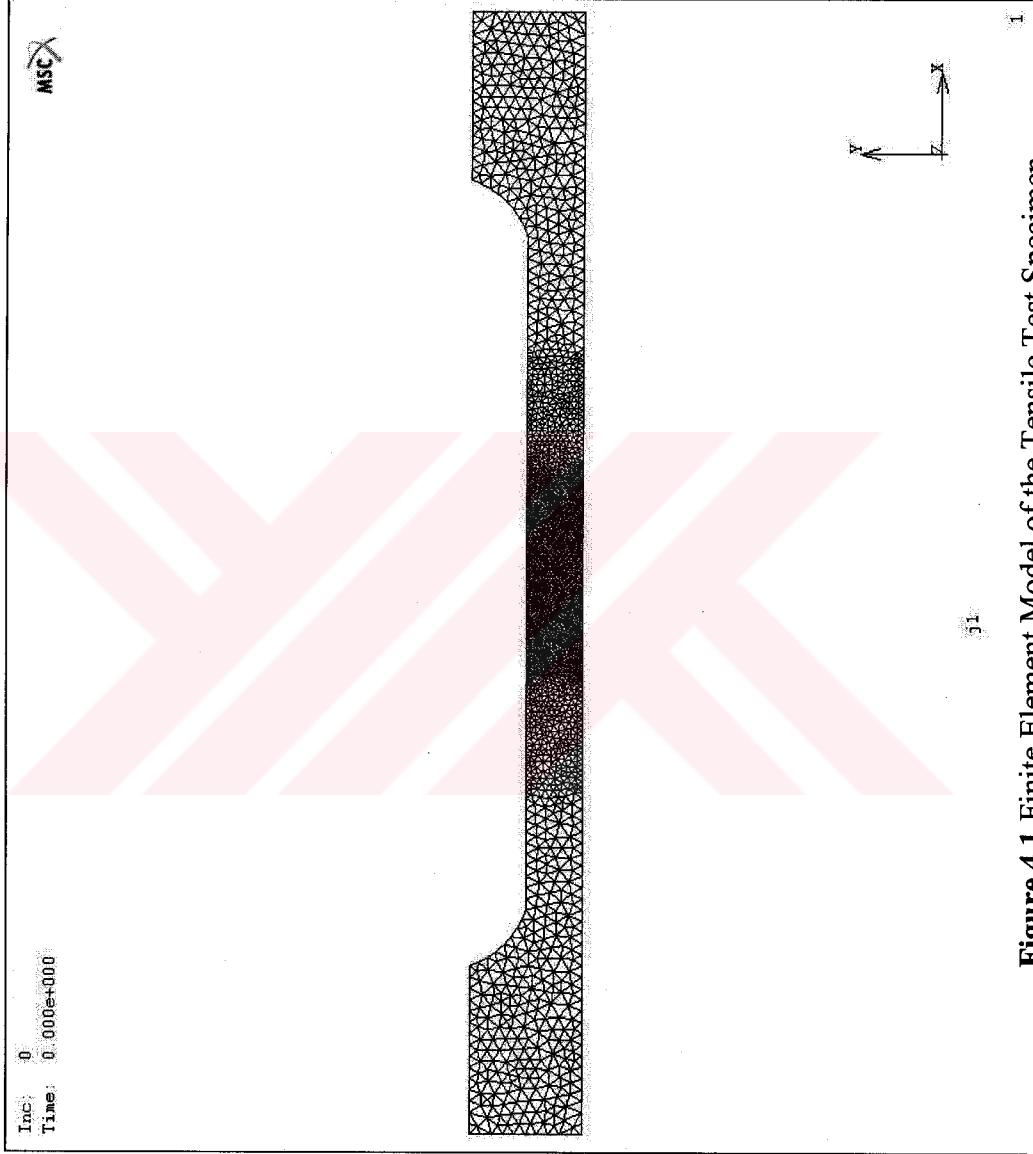


Figure 4.1 Finite Element Model of the Tensile Test Specimen

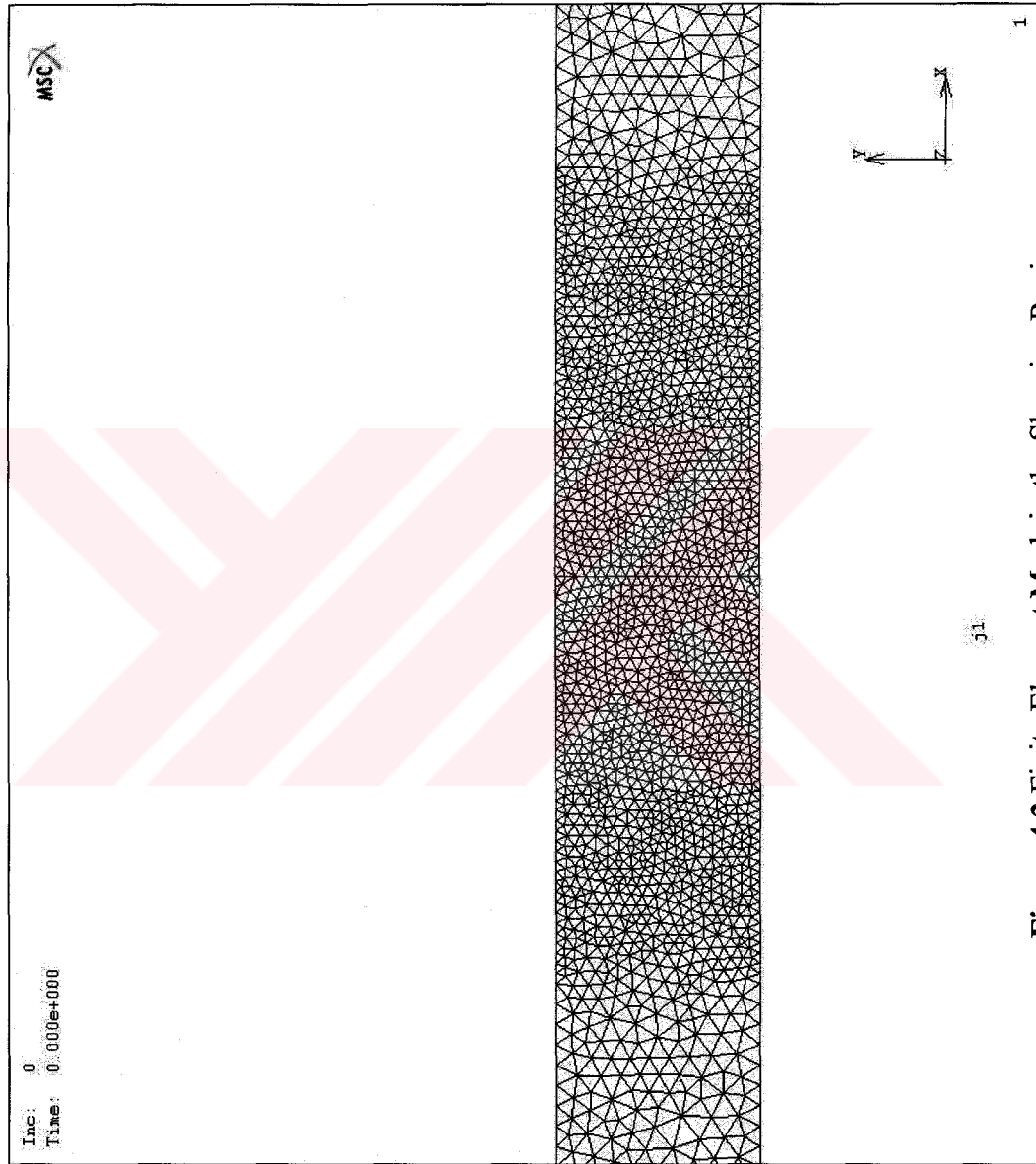


Figure 4.2 Finite Element Mesh in the Shearing Region

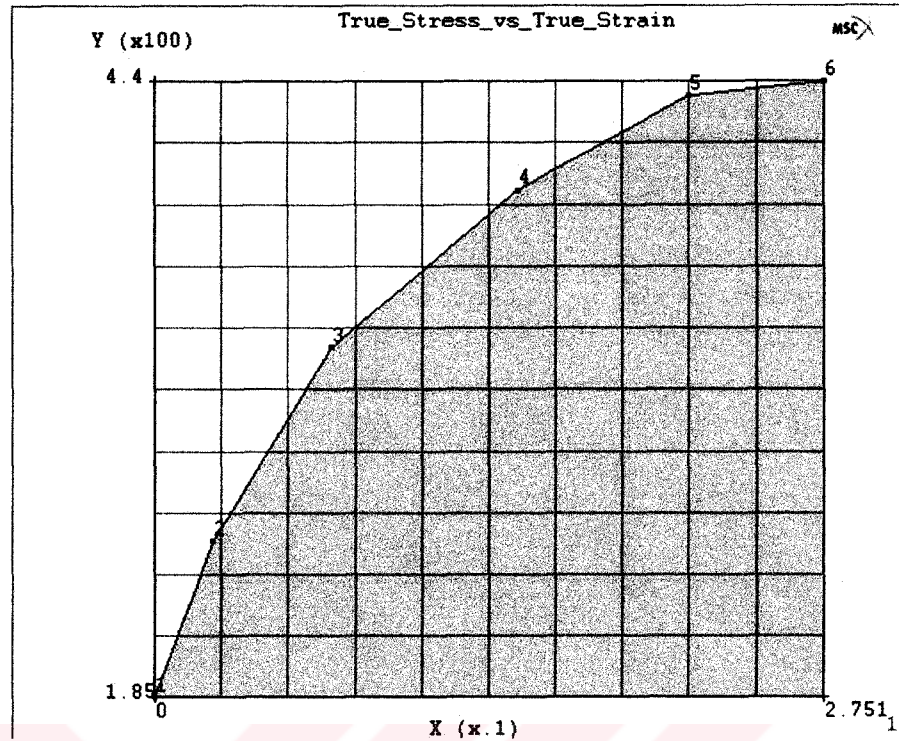


Figure 4.3 Stress-strain Graph Used in the Analysis

Material data obtained from actual tension tests are used in the finite element analysis (Figure 4.3).

Full Newton-Raphson method and updated Lagrangian approach are used as the solver options in the analysis. Element 125, which is a six node triangular plane strain element with full integration, is used [59].

Results of the analysis are given in Figure 4.4, 4.5, 4.6, 4.7. Figure 4.4 and 4.5 show the equivalent von Mises stress distribution in the specimen and around the point of failure, respectively. Figure 4.6 and 4.7 show the total equivalent plastic strain distribution.

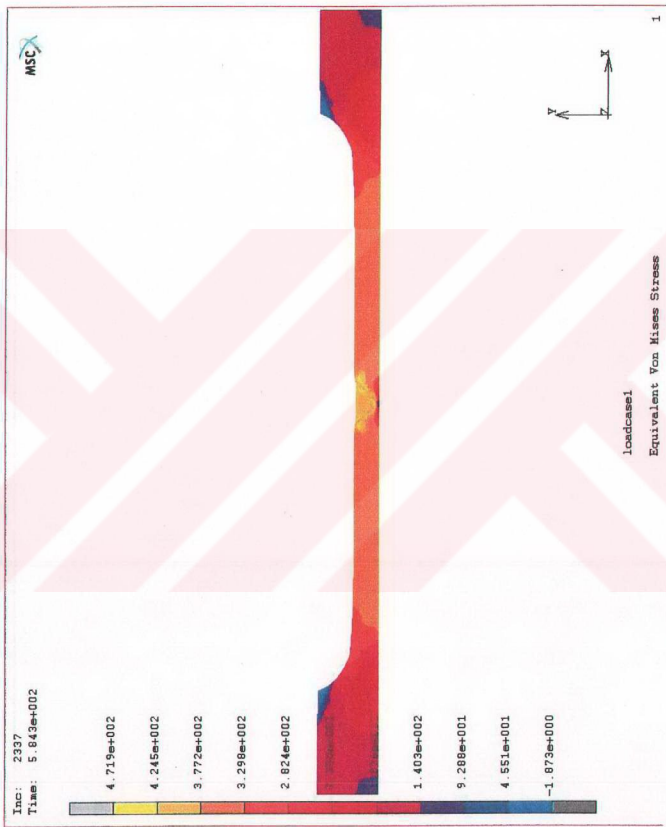


Figure 4.4 Stress Distribution at the Instant of Failure

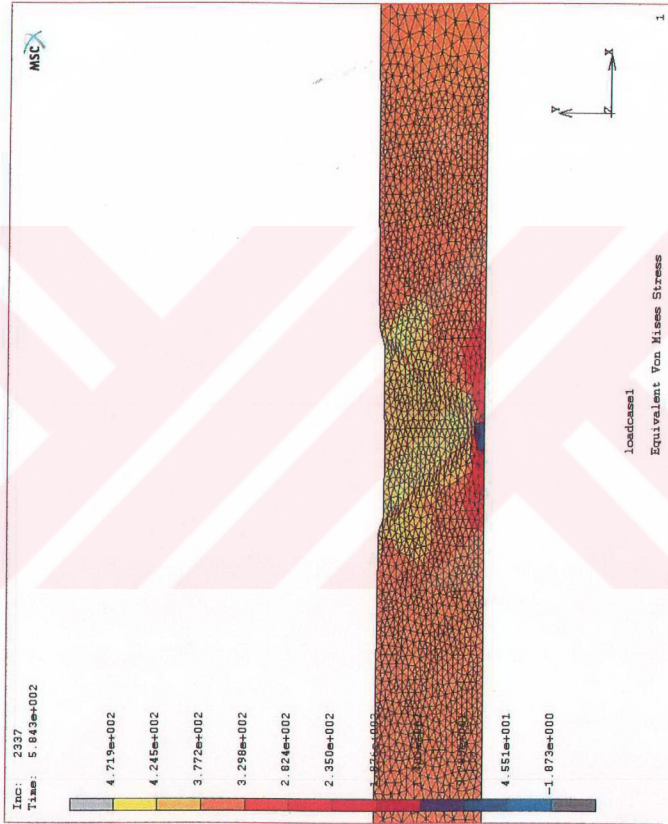


Figure 4.5 Stress Distribution At the Failure Region

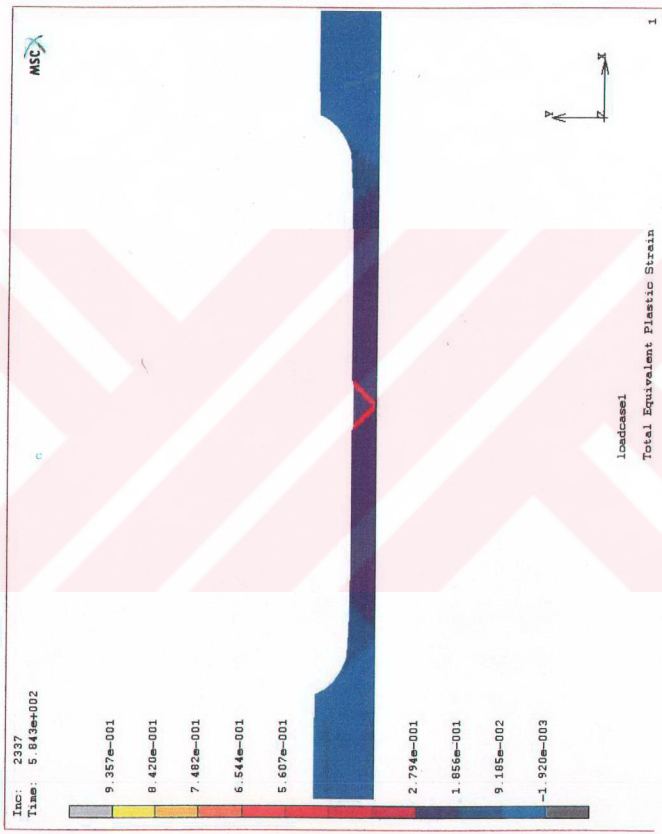


Figure 4.6 Equivalent Plastic Strain Distribution at the Instant of Failure



Figure 4.7 Plastic Strain Distribution at the Failure Region

The specimen failed in two shear planes which are approximately 45 degrees with respect to the longitudinal axis of the specimen. The finite element simulation resulted in two planes since it is an ideal model of the actual process. But in the actual tension test only one shear plane is observed because of the irregularities in the microstructure. These irregularities create weak points in the specimen and it fails in the weaker side.

Figure 4.8 is the true stress vs displacement graph drawn according to the data obtained from node 99 which is the node in the symmetry axis of the model. This node is chosen because it resides on the element that failed first. Numbers on the graph shows the increment number of the analysis. The graph is consistent with the results of the actual tension test that is given in Appendix B.

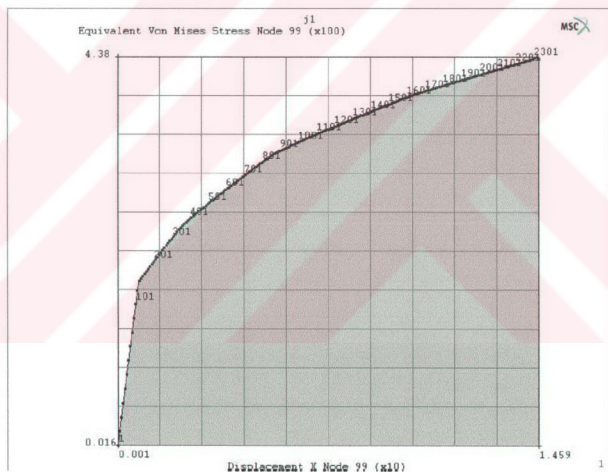


Figure 4.8 Equivalent von Mises Stress vs Displacement Graph of the Failed Element

Final lengths of the tension test specimens and results obtained from the analysis are given in Table 4.1.

TABLE 4.1 Results of the Analysis of Tension Test at Room Temperature

Specimen	Final Length (mm)	Percent Elongation	Error (%) with respect to analysis
0-deg rolling direction	227,3	13,65	0,79
45-deg rolling direction	229,8	14,9	0,30
90-deg rolling direction	226,2	13,1	1,28
Average	227,8	13,88	0,59
Simulation result	229,1	14,55	0,00

4.2 Simple Tension Test at Elevated Temperatures

Tension tests at high temperatures are done in order to determine material properties at high temperatures for the part analyzed in Chapter 5. Procedure of the tensile test and basic concepts are given in [62-68].

Statistical process control of the forging part analyzed in Chapter 5 – Case Study revealed that trimming operation is performed between 590 and 670C . Due to the capability of the tensile testing equipment used maximum temperature at which tensile tests could be done is limited to 450C . To be able to simulate the process realistically the material used in the finite element analyses are chosen from the material library of MSC.MARC. To insure the consistence of the mechanical properties of the material in hand and the material in the material library a series of “virtual” tension tests are done and results are compared with the actual test results. These virtual tension tests are done in 300C , 400C and

450C . Results of the analysis of these tests are given in Appendix C. Comparison of the test and simulation results are given in Table 4.2.

TABLE 4.2 Results of the Analysis of Tension Test at High Temperatures

Material	Temperature (C)	Ultimate Tensile Strength (MPa)	Initial Length (mm)	Final Length (mm)	Elongation (mm)	Percent Elongation
C45 MSC.MARC	300		50	53.29	3.29	6.58
C45 AKSAN	300	1093.0	45.6	49.5	3.9	8.5
C45 MSC.MARC	400		50	55.48	5.48	10.96
C45 AKSAN	400	839.1	46.3	52.3	6.0	12.9
C45 MSC.MARC	450		50	53.91	3.91	7.82
C45 AKSAN	450	678.0	45.4	49.2	3.8	8.4

CHAPTER V

CASE STUDY

Several forged parts have been examined and observations were done in the factory floor, and a hot forged part, which is used in the transmission of heavy-duty machinery, was chosen (Figure 5.1). The technical drawing of this part is given in Appendix D and the process flow chart is given in Table 5.1



Figure 5.1 The part used in case study

Table 5.1 Process Flow Chart for Part 198-290.2 [69]

PART NO: 198-290.2 PART NAME: SCHALTGABEL ROHTEIL CUSTOMER: USD			
OPERATION NO	PROCESS NAME	MACHINE TOOL	ALTERNATIVE MACHINE TOOL
10,00	Raw material control	-	
20,00	Die revision or manufacture	-	
30,00	Die control	-	
40,00	Raw material cutting	Automatic saw	
50,00	Attachment of dies to the machine tool	1000 tone press	
60,00	Material heating	100 kW induction furnace	
70,01	1. Preform (upsetting)	1000 tone press	
70,02	2. Preform (elongation)	1000 tone press	
70,03	3. Preform (flattening)	1000 tone press	
70,04	4. Preform (final shape stage 1)	1000 tone press	
71,00	Final shape (stage 2)	1000 tone press	
73,00	Trimming	250 tone press	100 tone press
74,00	Hot ironing	250 tone press	
80,00	Sandblasting	-	
130,01	Heat treatment	-	
170,00	Grinding (if necessary)	-	
180,00	Final control	-	
190,00	Packaging, labeling, shipment	-	

5.1 Manufacturing of the Part

The material properties of the part and the tension test results at room temperature and at elevated temperatures are given in Appendix C. Statistical process data collected during manufacturing is given in Appendix E. Statistical process control study was done for three critical dimensions, which are the dimensions designated by 5, 9 and 12 a, on the part (Figure D.1) to determine problematic regions of the part. Flash formation and the quality of the trimming surface were also observed. In practice, surface of the trimming die, especially around the cutting edge is filled with a special type of welding to obtain extra durability and long lasting dies. Properties of this electrode are given in Appendix F. Temperatures before and after the trimming operation were measured by special measuring equipment. Properties of this device are given in Appendix G.



Figure 5.2 Manufacturing steps of the forging 198-290.2

The part is manufactured in eight steps. Figure 5.2 shows first seven steps of the manufacturing. In the eighth step, the part is pressed in a 250-tonne press to flatten the slight warping in the part and reduce the thickness of the part into the desired tolerances. Manufacturing of the part was completed in five sets of dies. These are: upsetting die, preform die, forging die, trimming die, and ironing die. First three of these dies are seen in Figure 5.4.a. Steps of manufacturing can be described as follows:

a) **Operations in Upsetting Die:**

Step 1: The raw material was heated up to 1100 C in an induction furnace. Temperature of the part was measured to be between 1050 to 1100 C at the exit from the furnace (Figure 5.3).



Figure 5.3 Heating of the part in the induction furnace (Step 1)

Step 2: The heated part was placed into the upsetting die (Figure 5.4.a). The length of the part was reduced by approximately thirty percent by the upsetting operation (Figure 5.4.b). Temperatures before the operation were around 950 C and between 550 to 600 C after the operation.

b) Operations in Preform Die:

Step 3: The part was formed by forging in three consecutive operations. It was rotated 90 degrees after each forging. Final length of the part was 35 to 40 percent longer and its diameter was reduced by 60 percent (Figure 5.5).

Step 4: One side of the circular material was flattened to be able to form the hook in the next step.

Step 5: The hook was shaped in the preform die (Figure 5.7).



Figure 5.4.a The heated part is placed into the upsetting die.

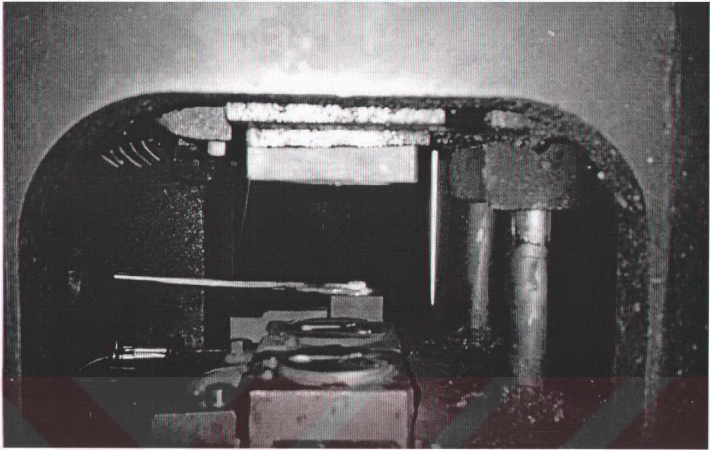


Figure 5.4.b Upsetting (Step2)

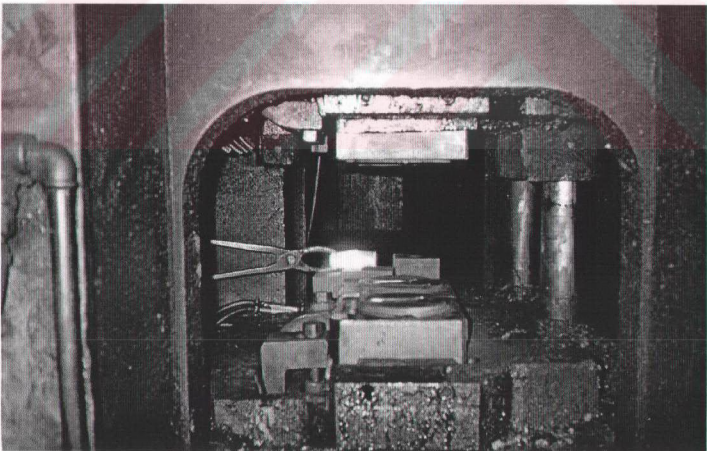


Figure 5.5 Part is elongated by forging in longitudinal axis (Step 3)

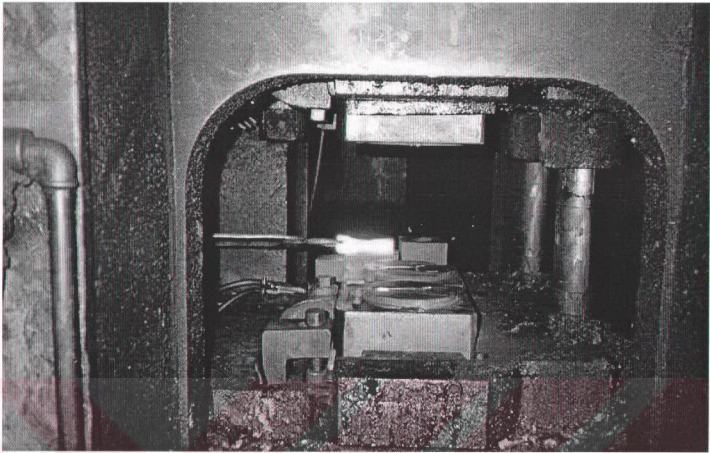


Figure 5.6 After Step 3 the part is forty percent longer



Figure 5.7 Preform forging (Step 4 - 5)

c) **Operation in the Forging Die:**

Step 6: The final shape was given to the part in the forging die including details such as the company name and part number (Figure 5.8).

d) **Operation in the Trimming Die:**

Step 7: The part was kept for 10-15 minutes in room temperature and then trimmed. Temperature of the part was at about 600-650 C during the trimming.

e) **Operation in the Correction Die:**

Step 8: Parts were compressed in a 250-tonne. This operation was necessary to flatten the slightly warped part, and reduce the thickness to desired dimensions.

Main problems related to the trimming operation in this part were excessive burr formation, high die wear, and premature die failure. The cutting surface generally had an irregular shape, and die and punch jamming occurred frequently because of this irregular form (Figure 5.9). A clearance of 0,8 mm was used in the trimming die instead of 1,5 mm [70], which is another reason of the jamming. Irregular residuals of burr formation were observed in the trimmed part at the bottom surface (Figure 5.10, Figure 5.11). These residuals were concentrated at the tips of the hook. Primary reason of these formations was high wear of the dies. After manufacturing 900 to 1000 parts it was necessary to maintain the trimming dies to satisfy quality requirements. These frequent stops in the manufacturing increased the production time and unit cost of the forging part reducing productivity and efficiency.



Figure 5.8 Final shape (Step 6)

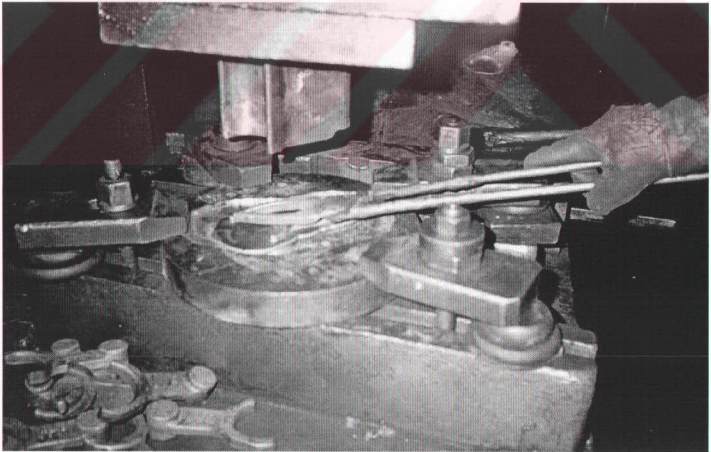


Figure 5.9 Inappropriate clearances caused jamming in trimming die



Figure 5.10 Trimming dies needed frequent maintenance



Figure 5.11 High wear rates in trimming dies increased down-time

5.2 Finite Element Simulation of the Trimming Operation

5.2.1 The Model

Figure 5.12 shows the 3D model of the trimming die. The die was modeled as a rigid body.

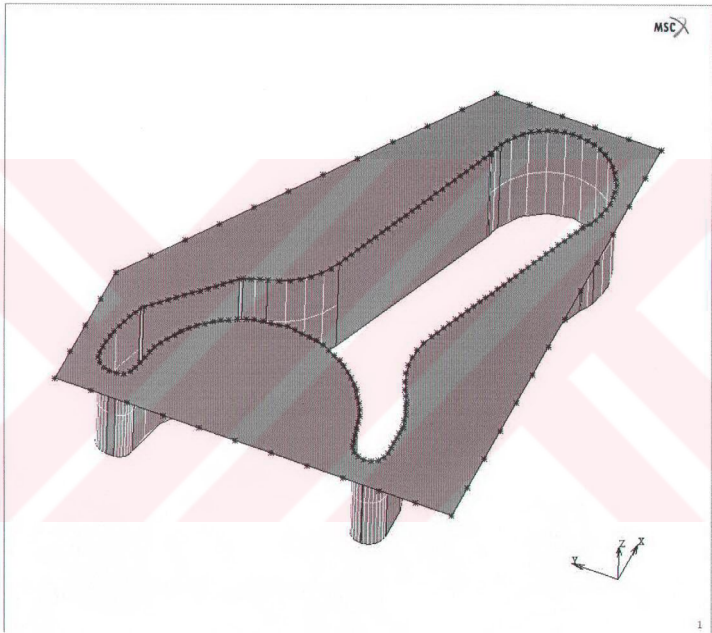


Figure 5.12 3D model of trimming die

The friction coefficient of the die was chosen as 0,5 [70]. During manufacturing, trimming of the actual part was done in room temperature with dies without any pre-heating. In the analysis initial temperature of the die was set to 20C°.

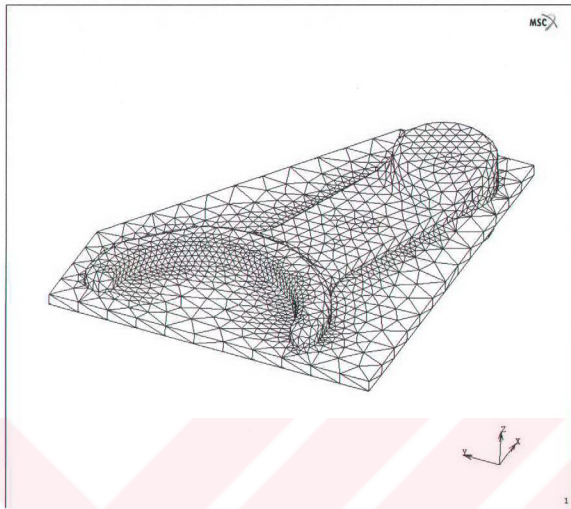


Figure 5.13 3D Finite element model of the workpiece

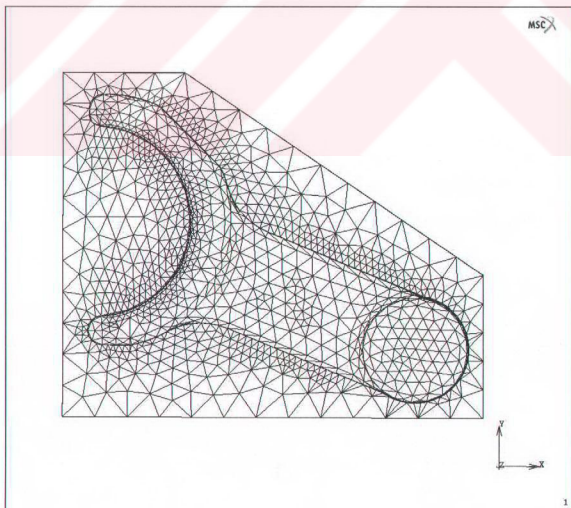


Figure 5.14 Finite element mesh is finer around the trimming region

Figure 5.13 and Figure 5.14 show the finite element model of the deformable body. Finite element mesh consisted of 25839 tetrahedral elements. The critical regions were modeled by a finer mesh.

5.3 Finite Element Analysis of Trimming

At first, the manufacturing process applied by the company was modeled. The analyses were run with the element elimination subroutine which is explained in Chapter 3. Analysis of the current practice showed the possible causes of problems. Figure 5.15 and Figure 5.16 show the part before the shearing process. Stress is concentrated around the trimming region as expected. This concentration of stress continued throughout the process until the flash was completely separated. Maximum value of the stress was obtained as 682.7 MPa in the tip of the hook. No plastic deformation was observed in this step. Figure 5.17 and Figure 5.18 show the plastic strain distribution in the part after the trimming was completed. Maximum value of the deformation is determined as 0,09585 in the lower tip as shown in Figure 5.18. The high stress concentration in the part at the end of the shearing process results in excessive wear in the trimming die at the tips of the hook. Statistical process control showed that this wear becomes imminent after 900 to 1000 parts were manufactured. Then excessive burr formation at the cutting surface, irregular cut surface and residuals of burr formation at the bottom surface and also premature die failures were observed.

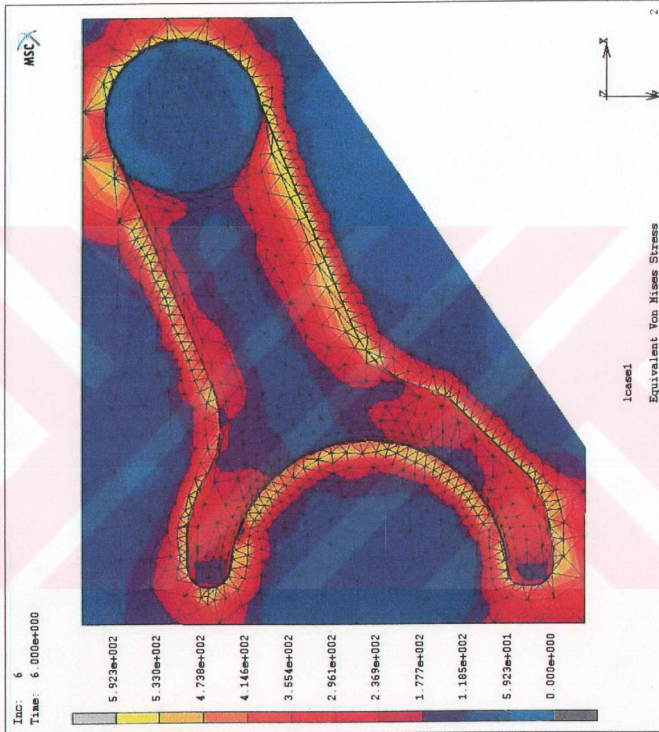


Figure 5.15 Top view of stress distribution of the workpiece in unmodified die

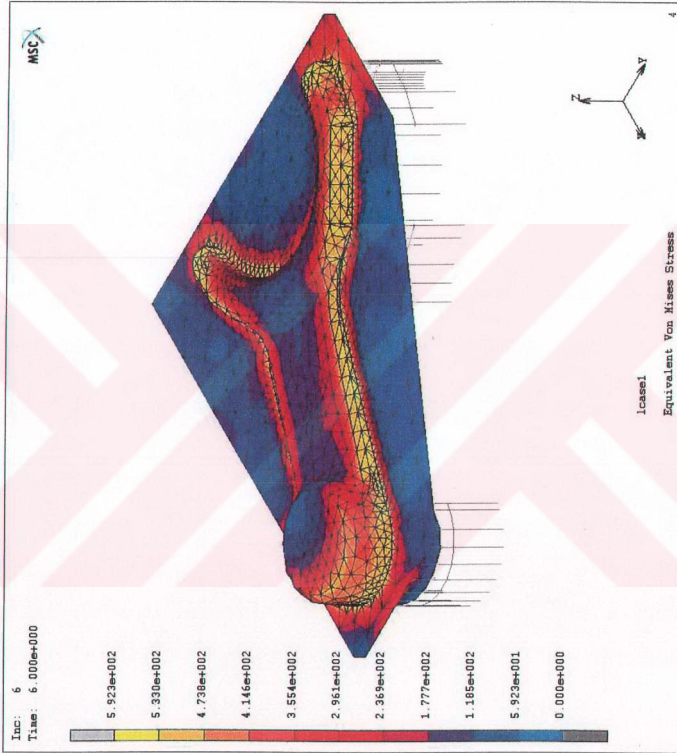


Figure 5.16 Perspective view of stress distribution of the workpiece in unmodified die

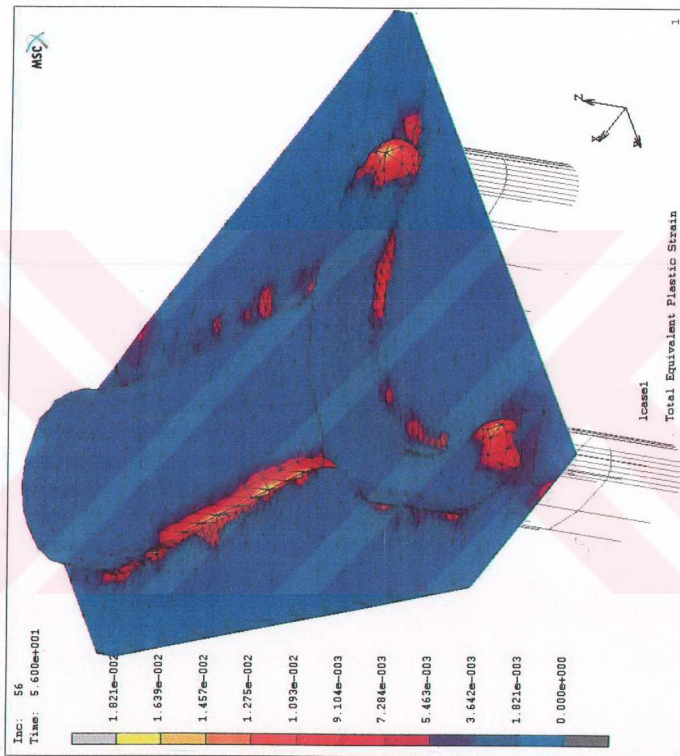


Figure 5.17 Plastic strain distribution of the workpiece in unmodified die

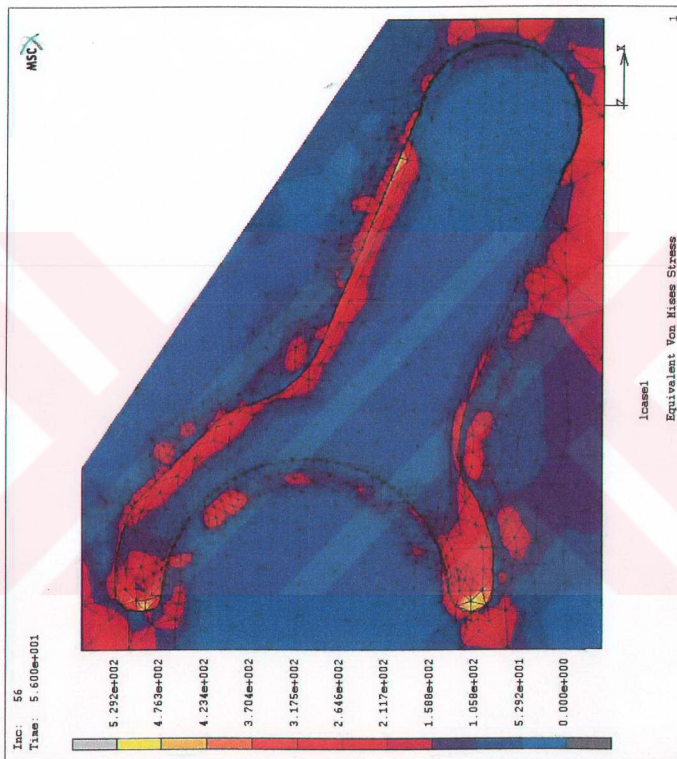


Figure 5.18 Plastic strain distribution of the workpiece in unmodified die

5.4 Finite Element Analysis of Trimming with Modified Die Set

After determining the distribution of stress and plastic strain, efforts were concentrated to reduce and eliminate the stress concentration by changing the geometry of the trimming die. Numerous simulations were run based on trial-and-error process, and different die angles were analyzed to find out the best angle which gave the minimum stress concentration in the tips of the hook. Table 5.2 gives the results obtained by changing the angle of the trimming die with respect to the horizontal surface. It was found that minimum stress levels were obtained when the angle between the die and the punch was 4° (Figure 5.19). Figure 5.20 shows the side view of the finite element model of the new design. At this configuration maximum equivalent von Mises stress was calculated as 541.2 MPa which indicated a reduction of 20.7% with respect to the current application without any angle. Maximum equivalent plastic strain was calculated as 0.01792, which was 81.3% less than the value obtained for parallel die and punch surfaces.

TABLE 5.2 Results of the Analysis

Die Angle (deg)	Max Equivalent von Mises Stress (Mpa)	Percent change of stress with respect to 0	Max Equivalent Plastic Strain	Percent change of plastic strain with respect to 0
0	682.7	0	9.585E-02	0
1	671.1	-1.7%	9.086E-02	-5.2%
2	632.1	-7.4%	6.981E-02	-27.1%
3	597.5	-12.5%	6.031E-02	-37.4%
4	541.2	-20.7%	1.792E-02	-81.3%
5	559.8	-17.9%	3.038E-02	-68.3%
6	584.4	-16.8%	3.278E-02	-65.8%

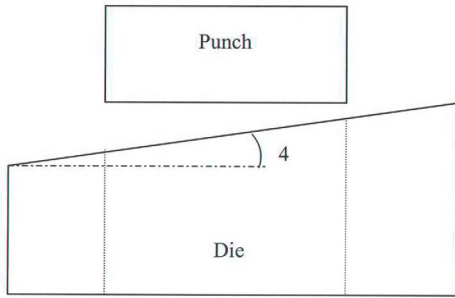


Figure 5.19 Modification in the trimming die

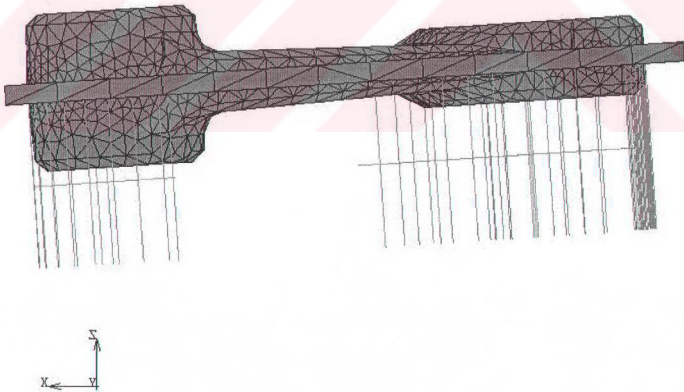


Figure 5.20 Model of workpiece in modified die

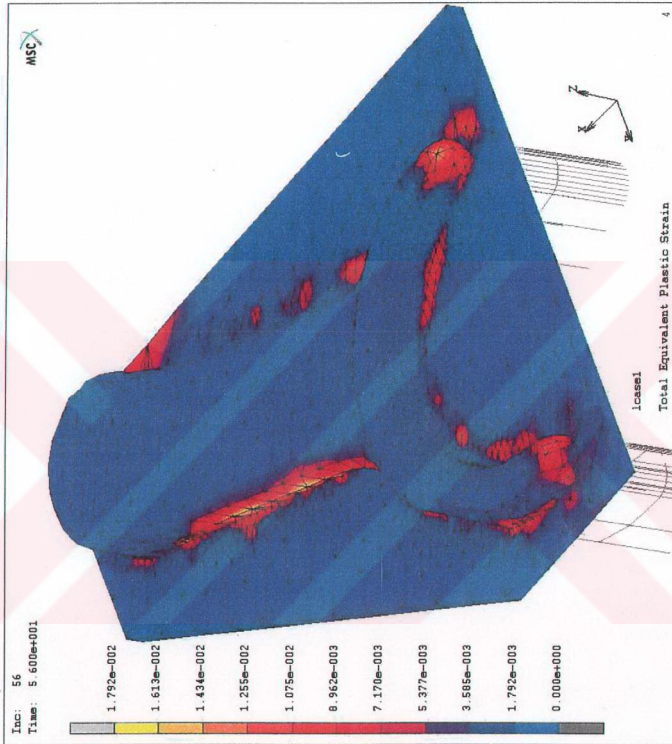


Figure 5.21 Plastic strain distribution of the workpiece in modified die

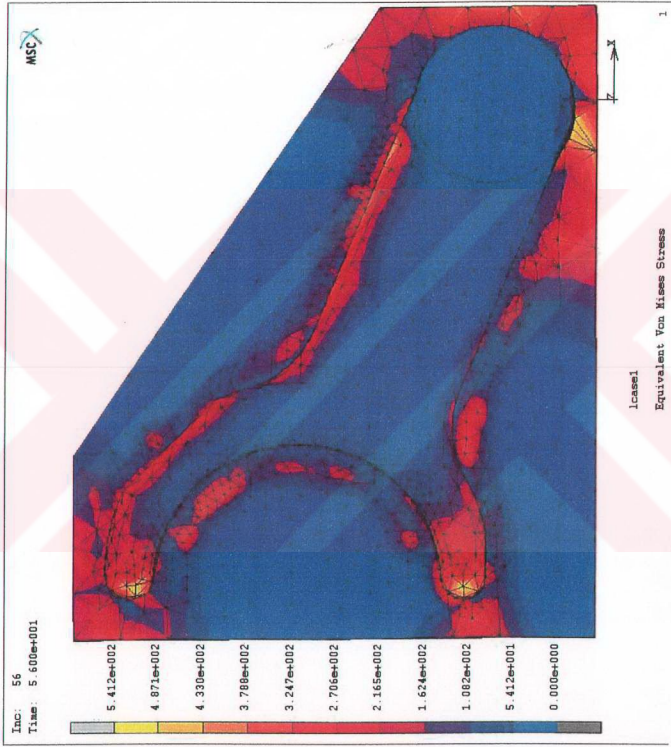


Figure 5.22 Plastic strain distribution of the workpiece in modified die

The model of the trimming die is not shown in the figure for clarity. Equivalent plastic strain distribution of the new design after the shearing was completed is given in Figure 5.21 and Figure 5.22.

5.5 Application of the New Design and Verification of the Analysis

The manufacturing process was stopped to maintain trimming dies after the production of one thousand parts because of irregular residuals of burr formation at the bottom surface of the part (Figure 5.23, Figure 5.24). Such parts are unacceptable and the manufacturing should be stopped to maintain trimming dies at this point. This worn out die set was used to verify the validity of this study in the light of the analysis done.



Figure 5.23 Side view of part with unacceptable flash residual.



Figure 5.24 Closer view of the defective region

To be able to use the available die set the end of the die, where the hook was placed, had been elevated by 3,6 mm to obtain an angle of 4° between the die and horizontal surface (Figure 5.26). Fifteen parts were produced with the modified die set. Figure 5.27, Figure 5.28, and Figure 5.29 show the results of the manufacturing with the modified die set. Parts does not have any burr formation and irregular cut surfaces and they satisfy the quality requirements.

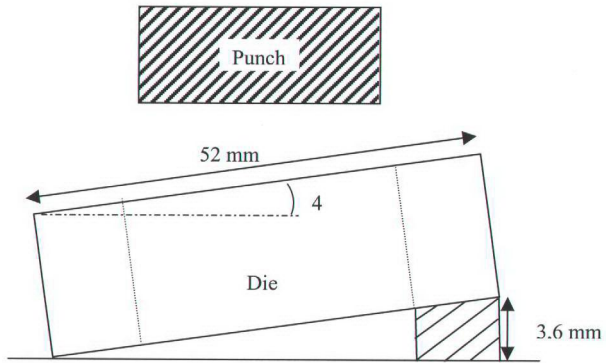


Figure 5.25 Schematic view of the application of die modification

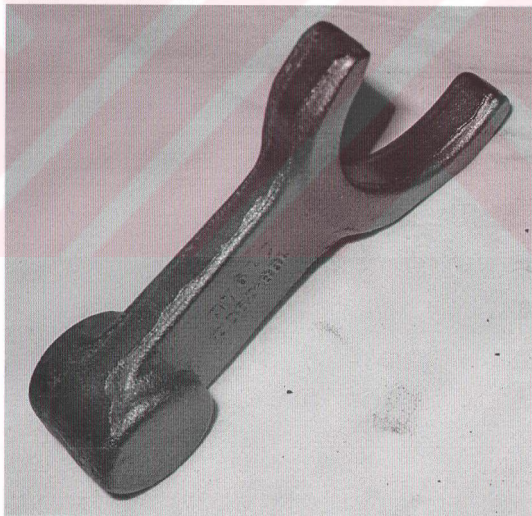


Figure 5.26 Part which was produced with the improved trimming die design



Figure 5.27 No irregular cutting surface or flash residual in new design

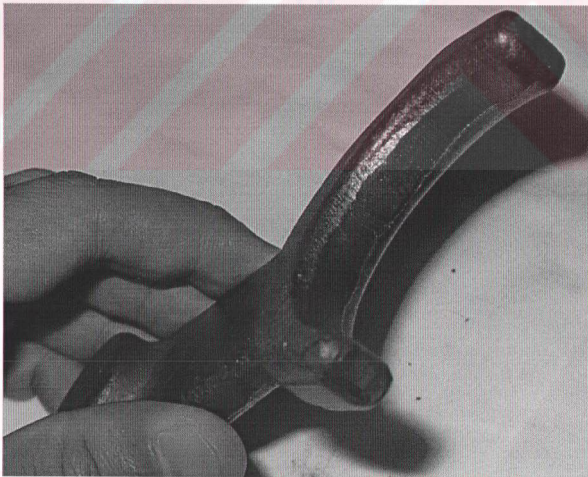


Figure 5.28 The cutting surface without any defect.

CHAPTER VI

DISCUSSION AND CONCLUSION

6.1 Conclusion

This study is focused on the simulation of trimming process by using the finite element method. A subroutine based on the element elimination method was developed for the commercial finite element code. Two failure criteria; shear strain energy density and effective plastic strain were used in the subroutine to predict failure.

Numerical results and experimental results were compared with simple tension tests conducted at room temperature. A good agreement has been observed.

A typical forged part was selected and analyzed by the finite element method and the problems encountered during trimming were investigated. Stress distributions were obtained and effects of several design changes on the stress concentrations were analyzed. It was numerically observed that stress levels could be decreased by modifying the trimming die. The modified die set was used in production of forged part and it is observed that the parts manufactured were in acceptable quality. As a result of this study quality of the forged part was improved and lifetime of trimming dies was increased.

6.2 Future Work

The other failure criteria which are summarized in Chapter 3 can be adapted to the user subroutine developed.

The trimming dies can be analyzed by using finer finite element mesh to reduce the mass lost because of the eliminated elements. It will also be possible to investigate the influence of clearance with a finer mesh.

The die set can be modeled by the finite element method and stress distribution in the dies can be analyzed to obtain longer die life.

The element elimination method can also be used with the help of the subroutine developed to analyze other manufacturing operations involving shearing such as blanking, piercing, etc.



REFERENCES

- [1] Altan, T., Vazquez, V., 1997, Status of Simulation Using 2D and 3D Finite Element Method. 'What is Practical Today? What Can We Expect In The Future?', Journal of Materials Processing Technology 71: 49 – 63.
- [2] Fujikawa, S., Ishihara, A., 1997, Development of Expert Systems for Forging Processes, JSAE Review 18: 127 – 133.
- [3] Fujikawa, S., 2000, Application of CAE for Hot-forging of Automotive Components., Journal of Materials Processing Technology 98: 176 – 181.
- [4] Li, G., Tinn, J.T., Wu, W.T., Oh, S.I., 2001, Recent Development of Three-dimensional Finite Element Modeling in Bulk Forming Processes, Journal of Materials Processing Technology 113: 40 – 45.
- [5] Vazquez, V., Altan, T., 2000, Die Design for Flashless Forging of Complex Parts, Journal of Materials Processing Technology 98: 81 – 89.
- [6] Breitting, J., Chemauskas, V., Taupin, E., Altan, T., 1997, Precision Shearing of Billets – Special Equipment and Process Simulation, Journal of Materials Processing Technology 71: 119 – 125.
- [7] Jirathearanat, S., Vazquez, V., Rodriguez, C.A., Altan, T., 2000, Virtual Processing – Application of Rapid Prototyping for Visualization of Metal Forming Processes., Journal of Materials Processing Technology 98: 116 – 124.

- [8] Özel, T., Altan, T., 2000, Process Simulation Using Finite Element Method – Prediction of Cutting Forces, Tool Stresses and Temperatures in High-speed Flat End Milling, *International Journal of Machine Tools and Manufacture* 40: 713 – 738.
- [9] Lin, Z.C., Lin, S.Y., 1992, A Coupled Finite Element Model of Thermo-Elastic-Plastic Large Deformation for Orthogonal Cutting, *Journal of Engineering Materials and Technology* 114: 218 – 228.
- [10] Strenkowski, J.S., Carrol, J.T., 1985, A Finite Element Model of Orthogonal Metal Cutting, *Journal of Engineering for Industry* 107: 349 – 354.
- [11] Komvopoulos, K., Erpenbeck, S.A., 1991, Finite Element Modeling of Orthogonal Metal Cutting, *Journal of Engineering for Industry* 113: 253 – 267.
- [12] Park, I.W., Domfeld, D.A., 2000, A Study of Burr Formation Processes Using the Finite Element Method: Part 1, *Journal of Engineering Materials and Technology* 122: 221 – 228.
- [13] Lin, C., Lo, P., 2001, 2D Discontinuous Chip Cutting Model by Using Strain Energy Density Theory and Elastic-plastic Finite Element Method, *International Journal of Mechanical Sciences* 43: 381 – 398.
- [14] Gouveia, B.P., Rodrigues, M.C., Martins, P.A., 1996, Fracture Predicting in Bulk Metal Forming, *International Journal of Mechanical Sciences* 38: 361 – 372.
- [15] Kim, H.S., Im, Y.T., Geiger, M., 1999, Prediction of Ductile Fracture in Cold Forging of Aluminum Alloy, *Journal of Manufacturing Science and Engineering* 121: 336 – 344.
- [16] MacCormack, C., Monaghan, J., 2001, Failure Analysis of Cold Forging Dies Using FEA, *Journal of Materials Processing Technology* 117: 209 – 215.
- [17] Creus, G.J., 2000, Instability and Damage Effects in the Modeling of Metal Forming, *Computer Methods in Applied Mechanical Engineering* 182: 421 – 437.

- [18] Peric, D., Vaz, M., Owen, D.R.J., 1999, On Adaptive Strategies for Large Deformations of Elasto-plastic Solids at Finite Strains: Computational Issues and Industrial Applications, *Computer Methods in Applied Mechanical Engineering* 176: 279–312.
- [19] Clift, S.E., Hartley, P., Sturgess, C.E.N., Rowe, G.W., 1990, Fracture Prediction in Plastic Deformation Processes, *International Journal of Mechanical Sciences* 32: 1–17.
- [20] Lee, S.W., Joun, M.S., 1999, Rigid-viscoplastic Finite Element Analysis of the Piercing Process in the Automatic Simulation of Multi-stage Forging Processes, *Journal of Materials Processing Technology* 104: 207–214.
- [21] Hambli, R., Potiron, A., 2000, Finite Element Modeling of Sheet-metal Blanking Operations with Experimental Verification, *Journal of Materials Processing Technology* 102: 257–265.
- [22] Hambli, R., 2001, Finite Element Model Fracture Prediction During Sheet-metal Blanking Processes, *Engineering Fracture Mechanics* 68: 365–378.
- [23] Taupin, E., Breitting, J., Wu, W.T., Altan, T., 1996, Material Fracture and Burr Formation in Blanking of FEM Simulations and Comparison with Experiments, *Journal of Materials Processing Technology* 59: 68–78.
- [24] Snape, R.G., Clift, S.E., Bramley, A.N., 1997, Sensitivity of Finite Element Analysis of Forging to Input Parameters, *Journal of Materials Processing Technology* 82: 21–26.
- [25] Breitting, J., Pfeiffer, B., Altan, T., Siegert, K., 1997, Process Control in Blanking, *Journal of Materials Processing Technology* 71: 187–192.
- [26] Fang, G., Zeng, P., Lou, L., 2001, Finite Element Simulation of the Effect of Clearance on the Forming Quality in the Blanking Process, *Journal of Materials Processing Technology* 122: 249–254.

- [27] Shuqin, X., Hoogen, M., Pyttel, T., Hoffmann, H., 2002, FEM Simulation and Experimental Research on the AlMg4.5Mn0.4 Sheet Blanking, *Journal of Materials Processing Technology* 122: 338 – 343.
- [28] Faura, F., Garcia, A., Estrems, M., 1998, Finite Element Analysis of Optimum Clearance in the Blanking Process, *Journal of Materials Processing Technology* 80 – 81: 121 – 125.
- [29] Maiti, S.K., Ambekar, A.A., Singh, U.P., Date, P.P., Narasimhan, K., 2000, Assessment of Influence of Some Process Parameters on Sheet Metal Blanking, *Journal of Materials Processing Technology* 102: 249 – 256.
- [30] Thomas, W., Oenoki, T., Altan, T., 2000, Process Simulation in Stamping – Recent Applications for Product and Process Design, *Journal of Materials Processing Technology* 98: 232 – 243.
- [31] Gözütübüyük, A.S., 1998, A Comparative Study on Computer Aided Modeling of Non-circular Deep Drawing, M.S. Thesis, Middle East Technical University, Ankara.
- [32] Mekarı, S., Mekarı, H., 1996, Analysis of Single-side Shearing by Using Punch with High Slenderness Ratio, *International Journal of Machine Tools Manufacturing* 37: 1109 – 1121.
- [33] Komori, K., 2001, Simulation of Shearing by Node Separation Method, *Computers and Structures* 79: 197 – 207.
- [34] Gillemot, L.F., 1976, Criterion of Crack Initiation and Spreading, *Engineering Fracture Mechanics* 8: 239 – 253.
- [35] Xu, S., Weinmann, K.J., 1997, On Predicting the Forming Limit Diagram for Automotive Aluminum Sheet, *Annals of the CIRP* 47: 177 – 180.
- [36] Zimniak, Z., 2000, Implementation of the Forming Limit Stress Diagram in FEM Simulations, *Journal of Materials Processing Technology* 106: 261 – 266.

- [37] Ohata, T., Nakamura, Y., Katayama, T., Nakamachi, E., Nakano, K., 1996, Development of Optimum Process Design System: by Numerical Simulation, Journal of Materials Processing Technology 60: 543 – 548.
- [38] Wilson, F., Harvey, P., Gump, C., 1955, Die Design Handbook, McGraw-Hill, London.
- [39] Thomas, W., Oenoki, T., Altan, T., 2000, Process Simulation in Stamping – Recent Applications for Product and Process Design, Journal of Materials Processing Technology. 98 (2000) 232-243.
- [40] Kim, H. S., Im, Y. T., Geiger, M., 1999, Prediction of Ductile Fracture in Cold Forging of Aluminum Alloy, Journal of Manufacturing Science and Engineering, Vol. 121 336–344.
- [41] Gillemot, L. F., 1976, Criterion of Crack Initiation and Spreading, Engineering Fracture Mechanics, Vol.8 (1976) 239–253.
- [42] Gouveia, B. P. P. A., Rodrigues, J. M. C., Martins, P. A. F., 1995, Fracture Predicting in Bulk Metal Forming, International Journal of Mechanical Sciences, Vol.38 (1996) 361–372.
- [43] Clift, S. E., Hartley, P., Sturgess, C. E. N., Rowe, G. W., 1989, Fracture Prediction in Plastic Deformation Processes. International Journal of Mechanical Sciences, Vol.32 (1990) 1-17.
- [44] Ceretti, E., Taupin, E., Altan, T., 1996, Simulation of Metal Flow and Fracture Applications in Orthogonal Cutting, Blanking, and Cold Extrusion, Annals of the CIRP Vol. 46 187 – 190

- [45] Lin, Z. C., Lo, S. P., 2000, 2-D Discontinuous Chip Cutting Model by Using Strain Energy Density Theory and Elastic-plastic Finite Element Method, *International Journal of Mechanical Sciences*, 43 (2001) 381-398.
- [46] Lee, S. W., Joun, M. S., 1999, Rigid-Viscoplastic Finite Element Analysis of the Piercing Process in the Automatic Simulation of Multi-stage Forging Processes, *Journal of Materials Processing Technology*, 104 (2000) 20 –214.
- [47] Park, I. W., Dornfeld D. A., 2000, A Study of Burr Formation Processes Using the Finite Element Method: Part 1, *Journal of Engineering Materials and Technology*, Vol.122 (2000), 221–228.
- [48] Komori, K., 2000, Simulation of Shearing by Node Separation Method, *Computers and Structures*, Vol.79 (2001) 197–207.
- [49] Güneş, A. T., *Pres İşleri Tekniği*, TMMOB Makina Mühendisleri Odası, MMO Yayın No: 129, 1987
- [50] Altan, T., Vazquez, V.,1997, Status of Simulation Using 2D and 3D Finite Element Method. ‘What is Practical Today? What Can We Expect In The Future?’, *Journal of Materials Processing Technology* 71: 49–63.
- [51] Breitting, J., Chemauskas, V., Taupin, E., Altan, T., 1997, Precision Shearing of Billets – Special Equipment and Process Simulation, *Journal of Materials Processing Technology* 71: 119 –125.
- [52] Johnson, W., Mellor, P. B., 1963, *Engineering Plasticity*, Van Nostrand Reinhold Company, London.
- [53] Clift, S.E., Hartley, P., Sturgess, C.E.N., Rowe, G.W., 1990, Fracture Prediction in Plastic Deformation Processes, *International Journal of Mechanical Sciences* 32: 1 – 17.

- [54] Gouveia, B.P., Rodrigues, M.C., Martins, P.A., 1996, Fracture Predicting in Bulk Metal Forming, *International Journal of Mechanical Sciences* 38: 361 – 372.
- [55] Park, I.W., Domfeld, D.A., 2000. A Study of Burr Formation Processes Using the Finite Element Method: Part 1, *Journal of Engineering Materials and Technology* 122: 221 – 228.
- [56] Lin, C., Lo, P., 2001, 2D Discontinuous Chip Cutting Model by Using Strain Energy Density Theory and Elastic-plastic Finite Element Method, *International Journal of Mechanical Sciences* 43: 381 – 398.
- [57] Lee, S.W., Joun, M.S., 1999, Rigid-viscoplastic Finite Element Analysis of the Piercing Process in the Automatic Simulation of Multi-stage Forging Processes, *Journal of Materials Processing Technology* 104: 207 – 214.
- [58] Kim, H.S., Im, Y.T., Geiger, M., 1999, Prediction of Ductile Fracture in Cold Forging of Aluminum Alloy, *Journal of Manufacturing Science and Engineering* 121: 336 – 344.
- [59] MARC User's Guide, Volume B-Element Library, MARC Analysis Research Corporation, 1996, 33-43.
- [60] MARC User's Guide, Volume A – Theory and User Information, MARC Analysis Research Corporation, 1996.
- [61] MSC.Marc User's Guide Volume C: Program Input, MARC Analysis Research Corporation, 1996.
- [62] Rastegaev, M.V., "New Methods of Homogeneous Compression of Specimens for the Determination of Flow Stress and the Coefficient of Internal Friction", *Zadov Lab.*, 1940, p.354
- [63] (Ed.) Lange, K., "Handbook of Metal Forming", McGraw Hill Book Company, New York, 1985.

- [64] Lenard, G. J., "Modelling Hot Deformation of Steels: An approach to understanding and behaviour", Springer-Verlag, Berlin, 1989.
- [65] Ilshner, B., "High Temperature Plasticity", Springer-Verlag, Berlin/Heidelberg/New York 1973.
- [66] Siebel, E., and Schwaigerer, S., "Mechanics of Tensile Test", Arch.Eisenhüttenwes., 19, 1949, pp.145-152.
- [67] Ludwik, P., "Elements of Technological Mechanics", Springer-Verlag, Berlin 1909.
- [68] Hollomon, J. H., "Tensile Deformation", Trans.AIME, 162, 1945, pp. 268-290.
- [69] AKSAN Forging Company, Esenboğa yolu 14. Km 06150 Ankara, Turkey
- [70] Wilson, F., Harvey, P., Gump, C., 1955, Die Design Handbook, McGraw-Hill, London, pp 5-1.
- [71] Özel, T., Altan, T., 2000, Process Simulation Using Finite Element Method – Prediction of Cutting Forces, Tool Stresses and Temperatures in High-speed Flat End Milling, International Journal of Machine Tools and Manufacture 40: 713 – 738.

APPENDIX A

SOURCE CODE OF THE USER-SUBROUTINE

```
RECURSIVE SUBROUTINE UACTIVE (IA, IB, IC, ID, IE, IFF, IG, IH)

      IMPLICIT REAL *8 (A-H, O-Z)

C   COMMON BLOCKS ARE ADDED

      include 'C:\MSC\marc2001\common\dimen'
      include 'C:\MSC\marc2001\common\lass'
      include 'C:\MSC\marc2001\common\creeps'
      include 'C:\MSC\marc2001\common\concom'
      include 'C:\MSC\marc2001\common\far'

C   START ELMVAR (Equ. Von Mises Stress) --- ARRAY IS
C   FORMED FOR THE CRITICAL VALUE

      DIMENSION EPTEN (NUMEL,6)

C   OUTPUT FILE IS OPENED FOR WRITING

      open(UNIT=13, FILE='output.txt', STATUS='OLD')

C   PARAMETERS ARE ASSIGNED ACCORDING TO THE TYPE OF
C   ANALYSIS

      KC=1
      ICODE=17
      IC=2

C   ELEMENT LOOP TO CHECK CRITICAL VALUE

      DO NN=1,6
      CALL ELMVAR (ICODE,N,NN,KC,EPTEN(N,NN))
      IC=2

      IF (EPTEN(N,NN) >= 440) THEN
```

```

C  CONDITION IS SATISFIED --- THE ELEMENT WILL BE
C  DELETED

      write(13,*) 'DELETED ',_INC, M, EPTEN(N,NN)
      IA=N
      IC=-1
      ID=1
      IE=1
      RETURN

      ELSE

C  CONDITION IS NOT SATISFIED --- ELEMENT WILL NOT BE
C  DELETED

      IC=2
      END IF

      END DO

      IC=2
      RETURN

      END

```

UACTIVE is written with the following headers:

```

SUBROUTINE UACTIVE
(M,N,MODE,IRSTSTR,IRSTSTN,INC,TIME,TIMINC)

      IMPLICIT REAL*8 (A-H,O-Z)
      DIMENSION M(2)

      "user coding"

      RETURN

      END

```

where:

M(1)	is the element number.
M(2)	is the master element number in an adaptive analysis
NN	is the internal element number.
MODE	-1 deactivate element. 2 leave in current status. 1 activate element.
IRSTSTR	set to 1 to reset stresses to zero.
IRSTSTN	set to 1 to reset strains to zero.
INC	is the increment number.
TIME	is the time at the beginning of the increment.
TIMINC	is the incremental time.

RECURSIVE command at the beginning of the subroutine enables the subroutine to be called within itself. This is necessary if an iterative solver is used in the solution.

INCLUDE command is used to contain specified libraries of MARC in the user-subroutine. These libraries are called "common blocks". Often, when using a user subroutine, more information is needed than is provided through the call arguments. Almost all information whether inputted in the pre-processing or calculated during the analysis is available through common blocks.

Explanation of each common block used in the sub-routine developed is given below. By "including" the common block the variables given next to the common block name are included in the calculations within the user-subroutine.

TABLE A.1: Common block description

COMMON BLOCK NAME	INCLUDED VARIABLE	EXPLANATION
dimen	NUMEL	Number of elements in mesh
	NUMNP	Number of nodes in mesh
	NDEG	Max number of degrees of freedom per node
	NCRD	Max number of coordinate directions
lass	N	ELSTO element number
	NN	Integration point number
	KC	Layer number
creeps	CPTIM	Time at beginning of increment
	TIMINC	Time increment
concom	INC	Increment number
	INCSUB	Subincrement number
far	M	Element number

After including the common blocks a two dimensional array is formed with the DIMENSION command. Size of this array is determined according to the properties of the finite element used as given in Equation 3.39.

The user subroutine writes the desired output to a text file. This is not necessary for the calculations and it does not affect the results. However, it is very convenient to see how the subroutine works especially in the code development stage. It also gives the user additional information on desired variables. This output file is opened for editing by the “open” command. “STATUS” command shows whether the file will be created by the user subroutine or it is an existing file.

Another utility routine of MARC is necessary to extract the solution results from the main solver in order to process them in the user subroutine during the analysis. ELMVAR utility routine is used to do this job.

A.1 ELMVAR Utility Routine

To facilitate extraction of solution results, it is possible to use the ELMVAR utility routine. This utility routine can be called from any user subroutine that is within an element loop. ELMVAR is used in conjunction with the MSC.MARC post element post codes to return the calculated values to the user subroutine.

ELMVAR is called with the following header:

```
CALL ELMVAR (ICODE, M, N, KC, VAR)
```

where:

ICODE	is the post code.
M	is your element number.
NN	is the integration point number.
KC	is the layer number.
VAR	is the current value(s) of the items requested.

If a tensor is requested, VAR should be a local array in the user subroutine, which is the case in the subroutine given here.

The values of ICODE determine which criterion is used in the failure analysis. If ICODE is set to 17 then equivalent von Mises stress will be returned, if ICODE is equal to 27 calculations will be done based on the effective equivalent plastic strain. The failure criteria can be set to a variety of other criteria by setting ICODE to other values. Complete list of ICODE values can be found in [61].

If the ELMVAR utility routine is called from a subroutine within the element assembly or stress recovery stage, the values of VAR are the current ones for this iteration. They are not necessarily the converged values.

After assigning appropriate values to the variables used by ELMVAR a DO loop is used to check every integration point of the element for critical values. Number of DO loops should be set according to the number of integration points in the element used. In the example given in Appendix A there are 9 integration points in the element used so DO loops recycle 9 times. Note that the subroutine is initiated from the beginning for every element; this means if there are 20000 elements in a model and the solution is obtained in 1000 time increments the subroutine is called 20000x1000 times during the solution. If an iterative solver is used this number depends on the number of iterations until convergence occurs. After the subroutine is called and the DO loop is entered ELMVAR utility routine obtains the value of the requested variable. This value is compared with the predetermined critical value. The critical value is 650 in the example, which is equal to the ultimate tensile strength of the material used. If the condition is satisfied the element is removed from the mesh, requested data is written to the output file and the analysis continues.

A.2 Sample Output

The user-subroutine works directly with the main solver and an output file is not necessary for the successful operation of the analysis. Contents of the output file do not influence the solution. However, an output file is formed for debugging reasons and to inform the user on the results of the analysis. The output file is in plain text format and the user can determine its contents easily by changing parameters in the subroutine. A sample of the output file of the user-subroutine is given below.

The first column represents the status of the finite element, second column is the increment number, the third column is the element number which has been deleted, and the fourth column shows the critical value, the equivalent von Mises stress in this case, at which the element is eliminated. Contents of the output file can be easily changed to obtain different variables due to the requirements of the analysis and to the interests of the user.

.
. .
. .

DELETED	1	20757	658.350052052368
DELETED	1	20825	658.919128669942
DELETED	1	22000	660.346015028578
DELETED	1	22003	661.587118270054
DELETED	1	22008	665.668277180789
DELETED	1	22795	652.597149642549
DELETED	1	22797	663.184621178984
DELETED	1	22798	674.955178347504
DELETED	1	22802	686.306930276222
DELETED	1	22804	666.352428186472
DELETED	2	553	663.579664911967
DELETED	2	1203	655.433818179867
DELETED	2	1240	690.014740301654
DELETED	2	1275	654.831642464813
DELETED	2	1382	660.571510741600
DELETED	2	1662	660.541945485619
DELETED	2	1663	651.796808406516
DELETED	2	1667	654.225047058575
DELETED	2	1830	663.488469285091
DELETED	2	1832	664.613513599980
DELETED	2	1851	661.774029888873
DELETED	2	1853	654.260638660885

. .
. .
. .

APPENDIX B

DATA AND RESULTS OF SIMPLE TENSION TEST AT ROOM TEMPERATURE



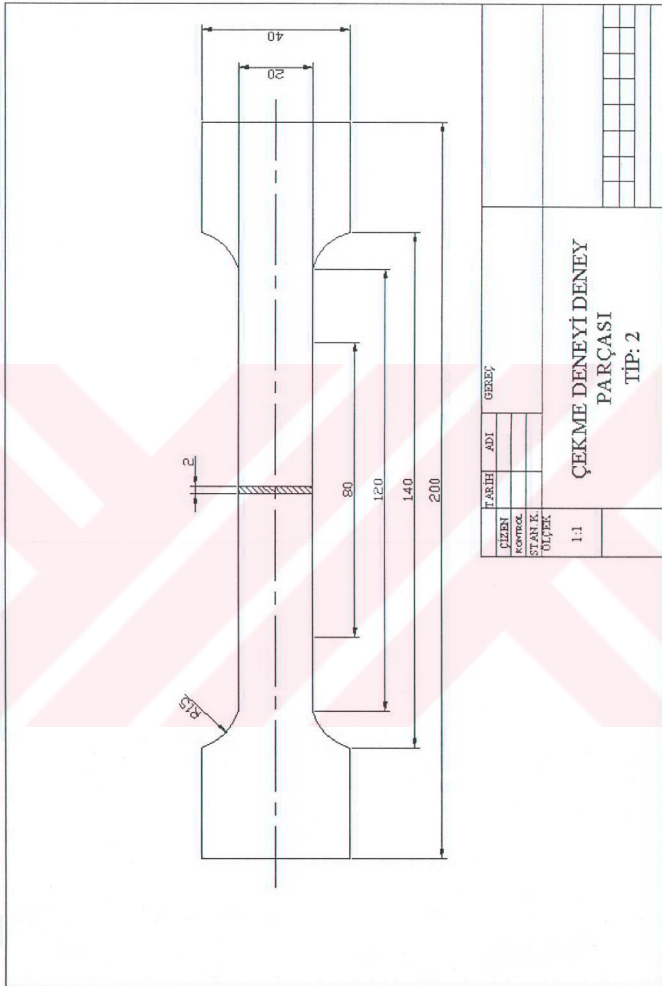


Figure B.1 – Technical Drawing of Test Specimen

B.1 Experimental Procedure

The numerical results are checked and verified by the experimental data obtained from the simple tension test at room temperature. Test specimens are prepared in three sets representing the 0°, 45°, and 90° with respect to the rolling direction. Dimensions of the test specimen and test results for the three set of specimen and the stress vs. strain graph are given in below. Mechanical properties of the material are interpolated from the following formula.

$$M_{ave} = \frac{M^o + 2M^{45} + M^{90}}{4} \quad (B.1)$$

True stress and corresponding true strain values are calculated by using the load versus elongation curve according to the following formulae:

$$\begin{aligned} \varepsilon_{true} &= \ln(\varepsilon_{eng} + 1) \\ \sigma_{true} &= \sigma_{eng} (\varepsilon_{true} + 1) \end{aligned} \quad (B.2)$$

where

$$\begin{aligned} \sigma_{eng} &= \frac{F}{A_o} \\ \varepsilon_{eng} &= \frac{l - l_o}{l_o} \end{aligned} \quad (B.3)$$

l is the current length and l_o is the initial length of the test specimen. F is the applied load and A_o is the initial cross sectional area. Young's Modulus value is calculated from the slope of the stress-strain curve.

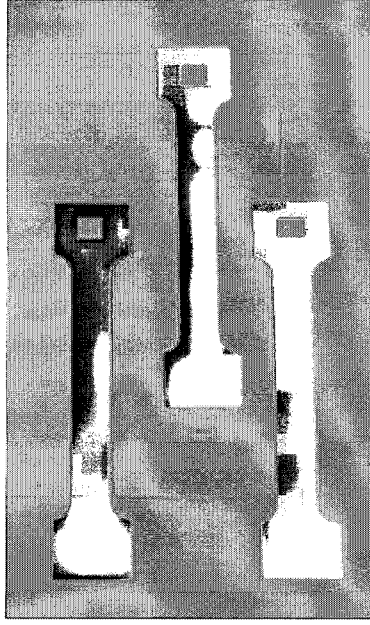


Figure B.2 Test specimens used in simple tension test

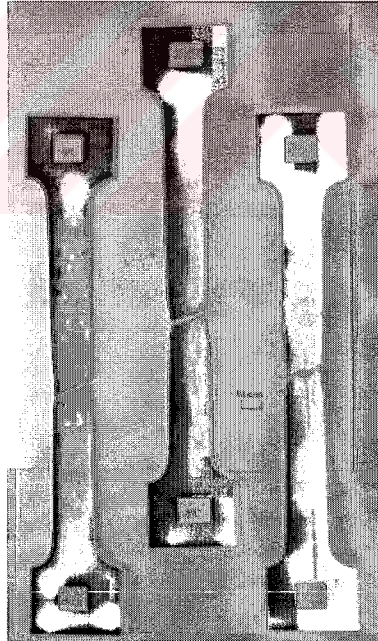


Figure B.3 Test specimens after the test

Table B.1

0 deg With Respect to Rolling Direction							
Load (kg)	Length (mm)	Area (mm ²)	Modified Load (N)	Eng. Stress (MPa)	Eng. Strain	True Strain	True Stress (MPa)
0,000	0,000	42,174	0,000	0,000	0,000	0,000	0,000
50,000	0,114	42,114	490,500	11,630	0,001	0,001	11,647
100,000	0,213	42,062	981,000	23,261	0,003	0,003	23,323
150,000	0,328	42,002	1471,500	34,891	0,004	0,004	35,034
200,000	0,445	41,940	1962,000	46,522	0,006	0,006	46,781
300,000	0,521	41,901	2943,000	69,782	0,007	0,007	70,237
400,000	0,597	41,861	3924,000	93,043	0,007	0,007	93,738
550,000	0,710	41,803	5395,500	127,934	0,009	0,009	129,071
700,000	0,823	41,744	6867,000	162,825	0,010	0,010	164,503
850,000	0,936	41,685	8338,500	197,717	0,012	0,012	200,034
1000,000	1,050	41,627	9810,000	232,608	0,013	0,013	235,664
1150,000	1,163	41,569	11281,500	267,499	0,015	0,014	271,392
1200,000	1,201	41,550	11772,000	279,129	0,015	0,015	283,324
1250,000	1,282	41,508	12262,500	290,760	0,016	0,016	295,423
1287,728	1,867	41,211	12632,612	299,536	0,023	0,023	306,536
1261,858	2,465	40,912	12378,828	293,518	0,031	0,030	302,574
1300,000	3,158	40,570	12753,000	302,390	0,040	0,039	314,343
1350,000	3,316	40,493	13243,500	314,020	0,042	0,041	327,054
1400,000	3,741	40,288	13734,000	325,651	0,047	0,046	340,900
1450,000	4,381	39,982	14224,500	337,281	0,055	0,053	355,773
1500,000	5,109	39,639	14715,000	348,912	0,064	0,062	371,222
1550,000	6,037	39,212	15205,500	360,542	0,076	0,073	387,781
1600,000	7,036	38,761	15696,000	372,172	0,088	0,084	404,945
1650,000	8,572	38,088	16186,500	383,803	0,107	0,102	424,980
1700,000	11,014	37,065	16677,000	395,433	0,138	0,129	449,941

Table B.1 (continued)

0 deg With Respect to Rolling Direction							
Load (kg)	Length (mm)	Area (mm ²)	Modified Load (N)	Eng. Stress (MPa)	Eng. Strain	True Strain	True Stress (MPa)
1710,000	11,572	36,839	16775,100	397,759	0,145	0,135	455,369
1720,000	12,257	36,565	16873,200	400,085	0,153	0,143	461,460
1730,000	13,420	36,109	16971,300	402,411	0,168	0,155	470,002
1740,000	14,474	35,706	17069,400	404,738	0,181	0,166	478,056
1750,000	15,456	35,338	17167,500	407,064	0,193	0,177	485,806
1760,000	20,012	33,727	17265,600	409,390	0,250	0,224	511,928
1750,000	22,066	33,047	17167,500	407,064	0,276	0,244	519,485
1740,000	23,369	32,630	17069,400	404,738	0,292	0,257	523,116
1730,000	24,583	32,251	16971,300	402,411	0,308	0,268	526,223
1720,000	25,023	32,116	16873,200	400,085	0,313	0,272	525,382
1710,000	25,338	32,020	16775,100	397,759	0,317	0,275	523,895
1700,000	25,605	31,939	16677,000	395,433	0,320	0,278	522,157
1650,000	26,433	31,690	16186,500	383,803	0,331	0,286	510,776
1600,000	27,090	31,495	15696,000	372,172	0,339	0,292	498,359
1587,335	27,300	31,434	15571,753	369,226	0,342	0,294	495,383

Table B.2

45 deg With Respect to Rolling Direction							
Load (kg)	Length (mm)	Area (mm ²)	Modified Load (N)	Eng. Stress (MPa)	Eng. Strain	True Strain	True Stress (MPa)
0,000	0,000	42,174	0,000	0,000	0,000	0,000	0,000
50,000	0,213	42,062	490,500	11,630	0,003	0,003	11,661
100,000	0,425	41,951	981,000	23,261	0,005	0,005	23,384
150,000	0,638	41,840	1471,500	34,891	0,008	0,008	35,169
200,000	0,851	41,730	1962,000	46,522	0,011	0,011	47,016
300,000	0,982	41,663	2943,000	69,782	0,012	0,012	70,639
400,000	1,064	41,620	3924,000	93,043	0,013	0,013	94,281
550,000	1,187	41,557	5395,500	127,934	0,015	0,015	129,833
700,000	1,310	41,494	6867,000	162,825	0,016	0,016	165,493
850,000	1,434	41,432	8338,500	197,717	0,018	0,018	201,260
1000,000	1,557	41,369	9810,000	232,608	0,019	0,019	237,134
1150,000	1,680	41,307	11281,500	267,499	0,021	0,021	273,116
1200,000	1,721	41,286	11772,000	279,129	0,022	0,021	285,134
1250,000	1,762	41,265	12262,500	290,760	0,022	0,022	297,164
1300,000	1,803	41,244	12753,000	302,390	0,023	0,022	309,206
1324,661	1,823	41,234	12994,920	308,126	0,023	0,023	315,149
1347,017	2,898	40,700	13214,239	313,327	0,036	0,036	324,677
1339,544	3,478	40,417	13140,927	311,588	0,043	0,043	325,133
1350,000	4,315	40,015	13243,500	314,020	0,054	0,053	330,959
1400,000	4,978	39,704	13734,000	325,651	0,062	0,060	345,913
1450,000	5,261	39,572	14224,500	337,281	0,066	0,064	359,462
1500,000	6,077	39,197	14715,000	348,912	0,076	0,073	375,415
1550,000	6,743	38,896	15205,500	360,542	0,084	0,081	390,929
1600,000	8,086	38,303	15696,000	372,172	0,101	0,096	409,788
1650,000	9,823	37,562	16186,500	383,803	0,123	0,116	430,928

Table B.2 (continued)

45 deg With Respect to Rolling Direction							
Load (kg)	Length (mm)	Area (mm ²)	Modified Load (N)	Eng. Stress (MPa)	Eng. Strain	True Strain	True Stress (MPa)
1700,000	12,196	36,595	16677,000	395,433	0,152	0,142	455,716
1710,000	12,877	36,327	16775,100	397,759	0,161	0,149	461,785
1720,000	13,585	36,052	16873,200	400,085	0,170	0,157	468,023
1730,000	14,353	35,759	16971,300	402,411	0,179	0,165	474,607
1740,000	16,127	35,099	17069,400	404,738	0,202	0,184	486,328
1750,000	20,439	33,592	17167,500	407,064	0,255	0,228	511,064
1740,000	24,983	32,138	17069,400	404,738	0,312	0,272	531,131
1730,000	26,094	31,801	16971,300	402,411	0,326	0,282	533,668
1720,000	27,013	31,528	16873,200	400,085	0,338	0,291	535,178
1710,000	27,542	31,373	16775,100	397,759	0,344	0,296	534,700
1700,000	27,850	31,284	16677,000	395,433	0,348	0,299	533,092
1650,000	28,761	31,021	16186,500	383,803	0,360	0,307	521,784
1600,000	29,547	30,799	15696,000	372,172	0,369	0,314	509,630
1583,639	29,800	30,728	15535,500	368,367	0,373	0,317	505,583

Table B.3

90 deg With Respect to Rolling Direction							
Load (kg)	Length (mm)	Area (mm ²)	Modified Load (N)	Eng. Stress (MPa)	Eng. Strain	True Strain	True Stress (MPa)
0,000	0,000	41,976	0,000	0,000	0,000	0,000	0,000
50,000	0,759	41,581	490,500	11,685	0,010	0,009	11,796
100,000	1,112	41,400	981,000	23,370	0,014	0,014	23,696
150,000	1,528	41,188	1471,500	35,056	0,019	0,019	35,726
200,000	1,833	41,035	1962,000	46,741	0,023	0,023	47,813
300,000	2,009	40,946	2943,000	70,111	0,025	0,025	71,875
400,000	2,080	40,911	3924,000	93,482	0,026	0,026	95,916
550,000	2,186	40,858	5395,500	128,538	0,027	0,027	132,054
700,000	2,292	40,805	6867,000	163,593	0,029	0,028	168,286
850,000	2,398	40,753	8338,500	198,649	0,030	0,030	204,611
1000,000	2,504	40,701	9810,000	233,705	0,031	0,031	241,029
1150,000	2,610	40,648	11281,500	268,761	0,033	0,032	277,540
1200,000	2,645	40,631	11772,000	280,446	0,033	0,033	289,731
1250,000	2,681	40,613	12262,500	292,131	0,034	0,033	301,932
1300,000	2,716	40,596	12753,000	303,816	0,034	0,033	314,144
1350,000	2,751	40,579	13243,500	315,502	0,034	0,034	326,366
1375,260	2,769	40,570	13491,301	321,405	0,035	0,034	332,544
1365,810	3,287	40,317	13398,596	319,197	0,041	0,040	332,329
1402,970	3,857	40,043	13763,136	327,881	0,048	0,047	343,708
1381,210	4,466	39,754	13549,670	322,796	0,056	0,054	340,839
1406,840	4,933	39,535	13801,100	328,786	0,062	0,060	349,087
1450,000	5,998	39,045	14224,500	338,872	0,075	0,072	364,311
1500,000	6,492	38,822	14715,000	350,557	0,081	0,078	379,041
1550,000	7,002	38,594	15205,500	362,243	0,088	0,084	393,990
1600,000	8,104	38,110	15696,000	373,928	0,101	0,097	411,856

Table B.3 (continued)

90 deg With Respect to Rolling Direction							
Load (kg)	Length (mm)	Area (mm ²)	Modified Load (N)	Eng. Stress (MPa)	Eng. Strain	True Strain	True Stress (MPa)
1650,000	9,312	37,594	16186,500	385,613	0,117	0,110	430,557
1700,000	11,233	36,802	16677,000	397,298	0,141	0,132	453,154
1710,000	11,767	36,588	16775,100	399,636	0,147	0,137	458,489
1720,000	12,380	36,345	16873,200	401,973	0,155	0,144	464,256
1730,000	12,994	36,104	16971,300	404,310	0,163	0,151	470,064
1740,000	13,699	35,833	17069,400	406,647	0,171	0,158	476,365
1750,000	14,542	35,512	17167,500	408,984	0,182	0,167	483,422
1760,000	15,740	35,068	17265,600	411,321	0,197	0,180	492,351
1770,000	19,846	33,624	17363,700	413,658	0,248	0,222	516,402
1760,000	22,525	32,745	17265,600	411,321	0,282	0,248	527,279
1750,000	23,316	32,494	17167,500	408,984	0,292	0,256	528,330
1740,000	23,784	32,347	17069,400	406,647	0,298	0,261	527,694
1730,000	24,130	32,240	16971,300	404,310	0,302	0,264	526,411
1720,000	24,404	32,155	16873,200	401,973	0,305	0,267	524,746
1710,000	24,631	32,085	16775,100	399,636	0,308	0,269	522,831
1700,000	24,833	32,023	16677,000	397,298	0,311	0,271	520,780
1650,000	25,843	31,717	16186,500	385,613	0,323	0,280	510,338
1634,240	26,200	31,611	16031,894	381,930	0,328	0,284	507,169

Stress - strain Diagram

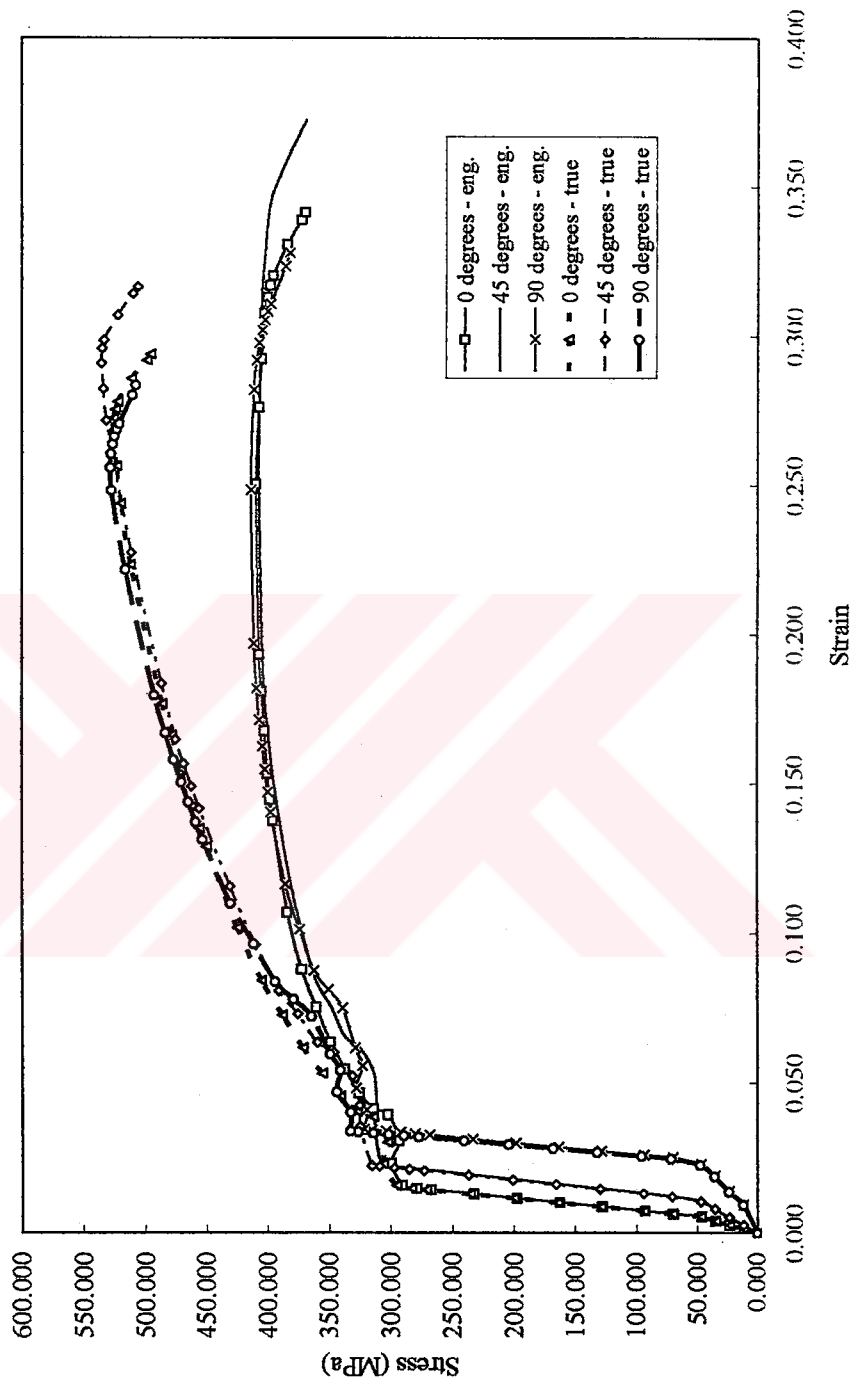


Figure B.5

APPENDIX C

Tension Test Results of C45 Material Used In Chapter 5

Original documents of spectral analysis and tensile testing report of the material are given in the following pages.



REPUBLIC OF TURKEY
MINISTRY OF INDUSTRY AND TRADE
SMIDO
SMALL AND MEDIUM INDUSTRY DEVELOPMENT ORGANIZATION
ANKARA CONSULTANCY AND QUALITY IMPROVEMENT CENTRE
CEVAT DÜNDAR STREET NO: 156 OSTİM/ANKARA
PHONE : 354 15 86-354 25 02 FAX : 354 54 85
E-mail : ostimdkgm@bir.net.tr

SPECTRAL ANALYSIS REPORT
(STEEL)

FORM NO : F-LAB 3.9.2.27
VALID FROM : July 1, 1998
REVISION NO : 00

FIRM NAME : AKSAN ÇELİK DÖVME

FIRM ADDRESS : ANKARA

APPLICATION DATE/NO : 04.01.2001

TESTING DATE : 05.01.2001

REPORT NO : 53

SAMPLE NO : 22/S= Ø28-834

SPECTRAL ANALYSIS VALUES

ELEMENT	%	ELEMENT	%	ELEMENT	%
CARBON (C)	0,4981	SILICON (Si)	0,200	MANGANESE (Mn)	0,697
PHOSPHOR (P)	0,0138	SULPHUR (S)	0,00753	CHROMIUM (Cr)	0,0865
MOLYBDENUM (Mo)	0,00363	NICKEL (Ni)	0,0552	ALUMINIUM (Al)	0,0175
COBALT (Co)	0,00877	COPPER (Cu)	0,131	NIObIUM (Nb)	<0,00275
TITANIUM (Ti)	0,00289	VANADIUM (V)	<0,00100	TUNGSTEN (W)	0,0102
LEAD (Pb)	<0,00200	TIN (Sn)	0,0105	ANTIMONY (Sb)	0,00734
IRON (Fe)	REST	MAGNESIUM (Mg)	-		

ANALYSED BY : NEVZAT EROL

APPROVED BY: BERİNNAZ ÇUHADAR
MEC.ENG.

EXPLANATIONS:

- 1) ANALYSE HAS BEEN CARRIED OUT ON THE SAMPLE GIVEN BY THE MENTION FIRM WITH THE "SPECTROLAB" SPECTROMETER INSTUMENT.
- 2) COPIES WHICH ARE NOT APPROVED BY SMIDO AS "IDENTICAL WITH ORIGINAL" ARE INVALID.
- 3) THIS REPORT IS ARRANGED AS 1 (ONE) PAGE

* OUR LABORATORIES HAS THE CERTIFICATE OF TS-EN-ISO 9002

20-12-00/3808

C45 - 300C°						
Load (kg)	Elongation (mm)	Area (mm ²)	Modified Load (N)	Engineering Stress (MPa)	Engineering Strain	True Stress (MPa)
0	0,1	24,618	0,000	0,000	0,002	0,000
250	1,8	23,746	2452,500	99,624	0,039	103,279
500	5,0	23,746	4905,000	199,248	0,104	206,559
750	7,5	22,891	7357,500	298,872	0,164	321,420
1000	10,0	22,891	9810,000	398,495	0,219	428,560
1250	12,2	22,051	12262,500	498,119	0,268	556,106
1500	14,0	22,051	14715,000	597,743	0,307	667,327
1750	19,0	20,418	17167,500	697,367	0,417	840,808
2000	26,5	20,418	19620,000	796,991	0,581	960,924
2100	29,0	18,848	20601,000	836,840	0,636	1093,016

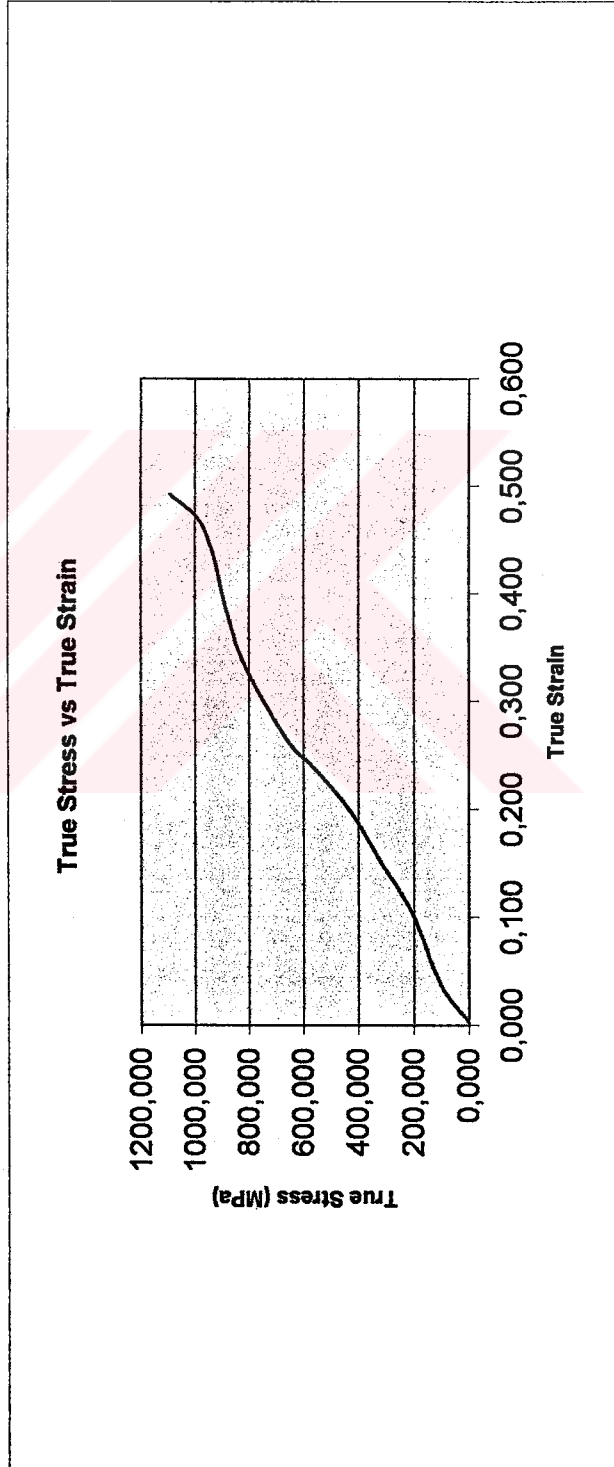


TABLE C.1 Tension Test Result at 300 °C

C45 - 400 C°							
Load (kg)	Elongation (mm)	Area (mm ²)	Modified Load (N)	Engineering Stress (MPa)	Engineering Strain	True Strain	True Stress (MPa)
0	0,0	25,505	0,000	0,000	0,000	0,000	0,000
250	3,0	25,505	2452,500	301,939	0,065	0,063	96,159
500	6,0	24,618	4905,000	603,878	0,130	0,122	199,248
750	8,8	23,746	7357,500	905,817	0,190	0,174	309,838
1000	11,5	22,891	9810,000	1207,756	0,248	0,222	428,560
1250	15,4	22,051	12262,500	1509,695	0,333	0,287	556,106
1500	23,0	21,226	14715,000	1811,634	0,497	0,403	693,240
1529	28,0	20,418	14999,490	1846,659	0,605	0,473	734,626
1450	36,5	18,848	14224,500	1751,247	0,788	0,581	754,701
1400	38,5	17,341	13734,000	1690,859	0,832	0,605	792,012
1350	39,9	15,896	13243,500	1630,471	0,862	0,622	833,121
1300	41,0	15,198	12753,000	1570,083	0,886	0,634	839,146

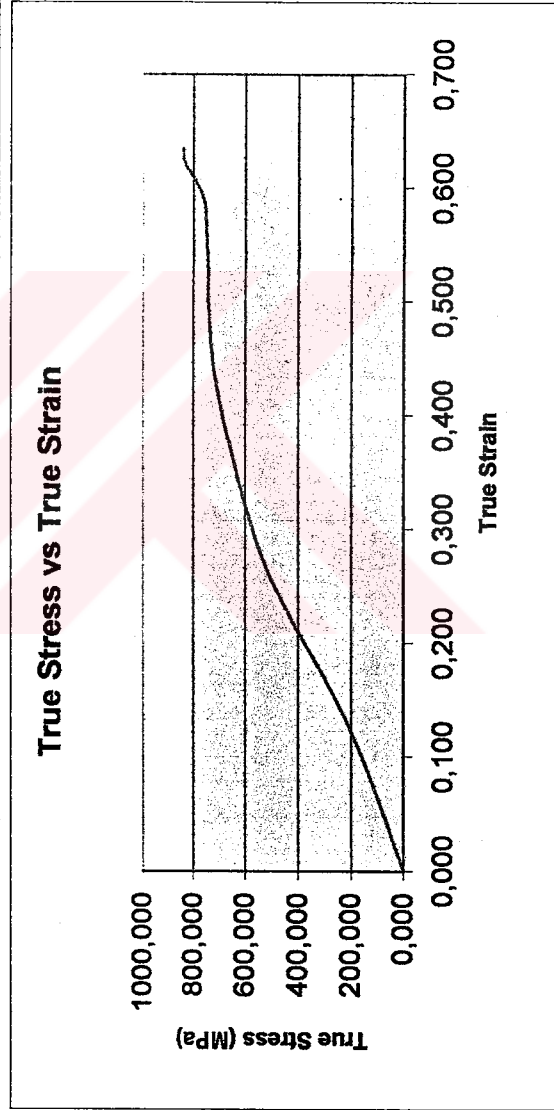


TABLE C.2 Tension Test Result at 400 °C

C45 - 450 C°							
Load (kg)	Elongation (mm)	Area (mm ²)	Modified Load (N)	Eng. Stress (MPa)	Engineering Strain	True Strain	True Stress (MPa)
0	0,1	23,746	0,000	0,000	0,002	0,002	0,000
250	2,5	22,891	2452,500	301,939	0,055	0,054	107,140
500	5,5	22,051	4905,000	603,878	0,121	0,114	222,442
750	8,5	21,226	7357,500	905,817	0,187	0,172	346,620
1000	12,0	20,418	9810,000	1207,756	0,264	0,235	480,462
1300	20,2	19,625	12753,000	1570,083	0,445	0,368	649,834
1340	23,5	18,848	13145,400	1618,393	0,518	0,417	697,448
1250	28,4	18,086	12262,500	1509,695	0,626	0,486	677,996

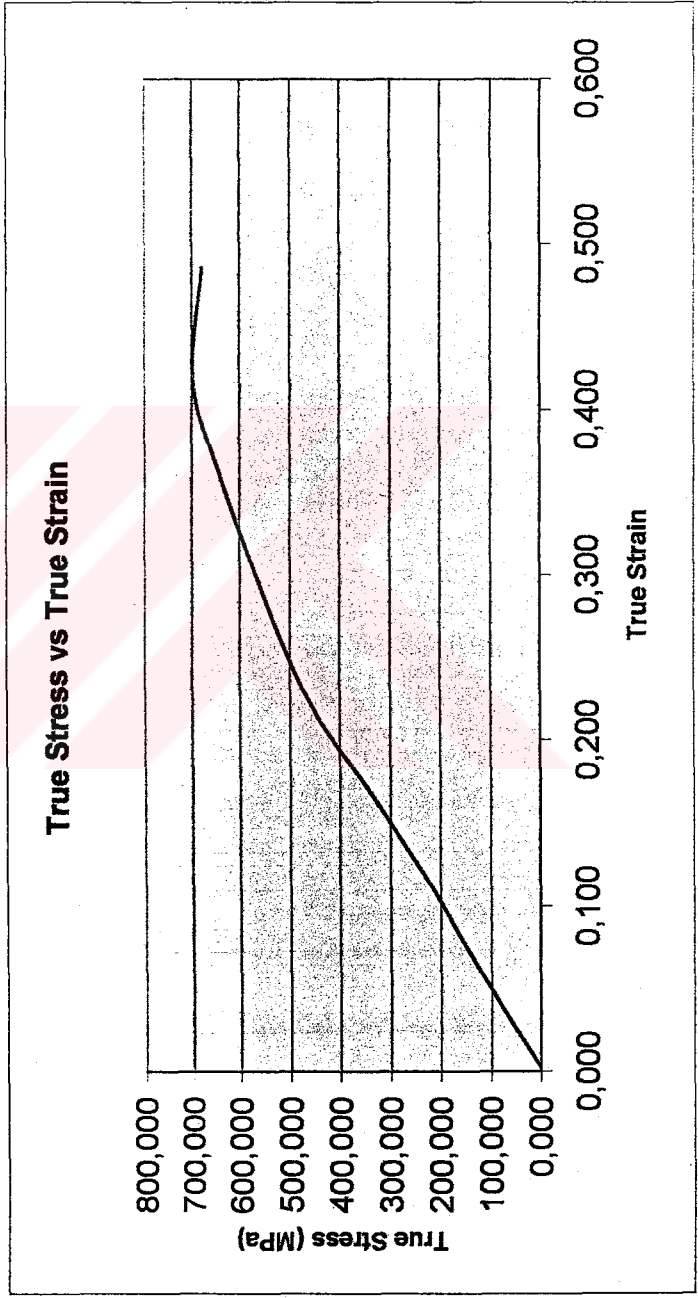


TABLE C.3 Tension Test Result at 450 °C

APPENDIX D

**TECHNICAL DRAWINGS OF AKSAN 198-290.2 AND TRIMMING
DIE SET**



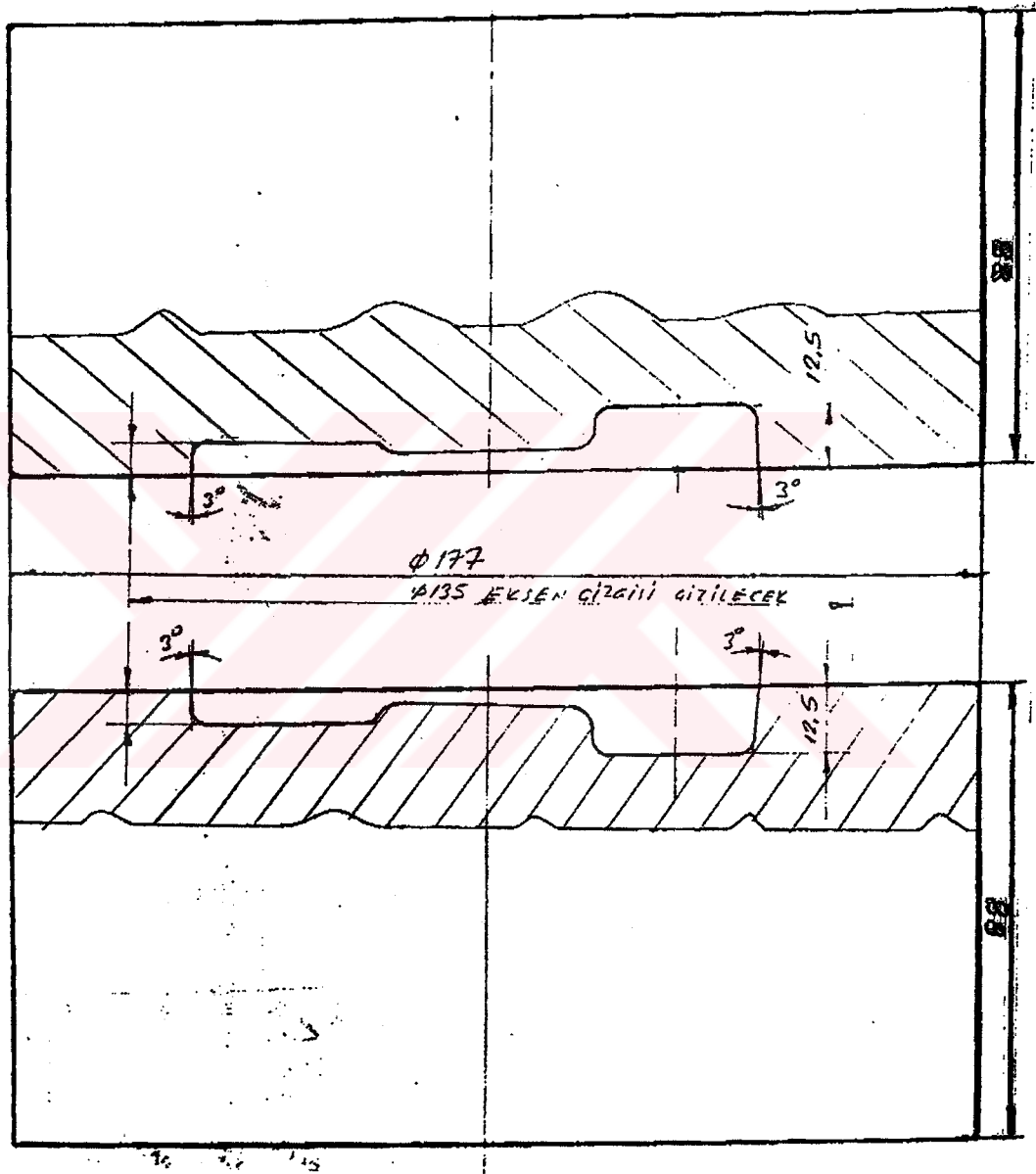


Figure D.2 – Technical Drawing of AKSAN 198-290.2 Trimming Die

APPENDIX E

SPC DATA

Statistical process control is used to observe variation of critical measures during manufacturing. With the help of this data wearing rates of the trimming die set is calculated. Measurement numbers are based on the technical drawing given in Appendix D – Figure D.1.



Table E.1 SPC Data of Workpiece Properties

Flash Thickness		Tolerance Range: 3,0 - 3,5 mm										Control Frequency					60 min			
Note: Measure from the center of hook		Number of Specimens: 5																		
Measurement	1	2	3	4	5	6	7	8	9	10	11	12	13	14	15	16	17	18	19	20
4,0																				
3,9																				
3,8																				
3,7					1		3	1			1									
3,6			2		1		1	1	1						2			1		1
3,5					1		1	1						1	1	2				1
3,4			1					2	2				1		1		2			1
3,3				2	2			1	1	1				2	1	1		2	1	1
3,2	1		1	2	1	1	1	1	2	2	1	2	1				1			2
3,1	1	1			1			1					1	1		1	2	1	1	
3,0	2	1		1					1	2	1	1	1		1	1				1
2,9		3	1			2			1				1	1						
2,8	1																			
2,7																				
2,6																				
2,5																				

Residual at the cut surface		Number of Specimens: 5										Control Frequency					60 min			
Note: Control visually																				
Present	1	2	3	4	5	6	7	8	9	10	11	12	13	14	15	16	17	18	19	20
							x		x	x					x		x	x	x	x
Not Present	x	x	x	x	x	x		x			x	x	x	x		x				

Temperature		Number of Specimens: 5										Control Frequency					60 min			
Note: Measure before and after the trimming																				
Before (C)	1	2	3	4	5	6	7	8	9	10	11	12	13	14	15	16	17	18	19	20
	654	670	630	665	620	641	649	638	675	620	660	650	654	643	622	676	643	662	637	611
	610	625	595	631	605	621	613	605	652	596	635	621	615	625	602	649	628	631	615	594

Table E.2 SPC Data of Dimension 5

Measurement Number	5 Tolerance Range					55 - 56.6					5 Control Frequency					60 min				
	1	2	3	4	5	6	7	8	9	10	11	12	13	14	15		16	17	18	19
Measurement	1	2	3	4	5	6	7	8	9	10	11	12	13	14	15	16	17	18	19	20
57,0																				
56,9																				
56,8																				
56,7																				
56,6																				
56,5																				
56,4																				
56,3																				
56,2																				
56,1																				
56,0									1	2										1
55,9						1	4	3	2	3										2
55,8			2			2	2	3	4	2					1	3	2	3	2	3
55,7	3	2	1	2	2	3	1	2	1	3		1	3	3	3	2	1	4		1
55,6	3	4	3	1	2	2	1	2	2		4	2	4	4	4	3	3	2	3	2
55,5	2	1	3	2	4	2	2				2	5	2	3	2	4	3	2	2	1
55,4	2	2	1	3	1						4	2	1		1					
55,3		1		1	1															
55,2				1																
55,1																				
55,0																				
54,9																				
54,8																				
54,7																				
54,6																				
54,5																				

Note: Both surfaces will be measured.

Table E.3 SPC Data of Dimension 9

Measurement Number:	9 Tolerance Range:	29,5 - 31,1	Number of Specimens:	5	Control Frequency:	60 min																
Note: Both surfaces will be measured.																						
Measurement	1	2	3	4	5	6	7	8	9	10	11	12	13	14	15	16	17	18	19	20		
32,0																						
31,9																						
31,8																						
31,7																						
31,6																						
31,5																						
31,4																						
31,3																						
31,2																						
31,1																						
31,0																						
30,9																						
30,8																						
30,7																						
30,6																						
30,5																						2
30,4																						2
30,3																						3
30,2	1																					1
30,1	1																					2
30,0																						
29,9	3	2	2	2	1	2	2	2	4	3	1	4	1	3	2	2	2	2	3	1		
29,8		2	3	1	3	4	3	1	1	2												
29,7	1	3	2	2	2	2	2		1													
29,6	2	1	3	3	1																	
29,5	1	2	1	2																		
29,4	1																					
29,3																						
29,2																						
29,1																						
29,0																						
28,9																						
28,8																						

APPENDIX F

PROPERTIES OF HARDFACING ELECTRODE

Hardfacing electrode
For metal/metal wear

HB 600 HT

Tip colour : Red

Classification *DIN 8555:* E3-UM-60-ST

**Description
and
applications**

Rutile coated electrode with a Cr-Mo-C martensitic steel deposit, resistant to metal/metal wear up to 550°C. For all pieces subject to hot or cold metal abrasion, even in presence of shocks and pressure. As welded only machinable by grinding.
Soft fusion, no spatters, self releasing slag.
Special applications: Hardfacing of shear blades, moulds, pressing and forging dies.

**All weld metal
mechanical
properties**

<i>Hardness</i>
58-61 HRC

Obtained in pour weld metal

Typical weld metal composition (%)	C	Si	Mn	Cr	Mo	Fe
	0.5	0.7	0.5	6.0	5.0	Rem

Packaging data	Size (mm)	2,5 X 350	3,2 X 350	4,0 X 450
	Electr./ packet	238	152	103
	Electr./ carton	952	608	412
	Kg 1000 electr.	21	33	63
	Packets / carton	4	4	4
	Kg / packet	5	5	6.5
	Kg / carton	20	20	26
	Amperes (A)	80	110	150

Welding instruction

Redrying, if necessary, 1h/250°C. Low alloyed, high carbon tool steels etc. have to be preheated to 250-450°C, depending on their composition and thickness. Slow cooling in still air after surfacing.

APPENDIX G

PROPERTIES OF TEMPERATURE MEASURING EQUIPMENT

SIEMENS ARDOPORT SERIES

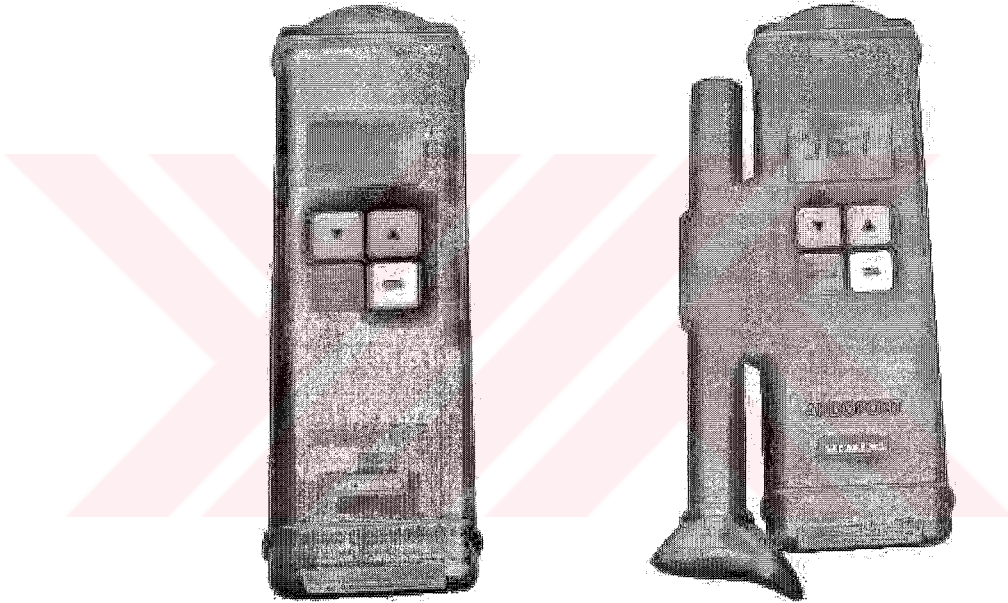


Figure G.1

- **Measurement range:** -30 ... 1999 °C (including contact sensor range)
- **Temperature resolution:** 1/10°C
- **Measurement accuracy:** 5% + 1 digit
- Built in memory for 64 measured values

- Capability to transfer measured values to a PC through serial port module
- The Ice- illumination or sighting aid with marking of measuring spot for the recognition by the correction of the value of the measuring spot
- Capable to measure temperature with contact and non-contact sensors.

